

Realism Control One-step Diffusion for Real-World Image Super-Resolution

Zongliang Wu^{1, 2, 3, *}, Siming Zheng^{3, *}, Peng-Tao Jiang^{3, #}, Xin Yuan^{2, #}

¹ Zhejiang University, Hangzhou, China

² School of Engineering, Westlake University, Hangzhou, China

³ vivo Mobile Communication Co., Ltd

* Equal contribution # Corresponding Author

{wuzongliang, xyuan}@westlake.edu.cn, {zhengsiming, pt.jiang}@vivo.com

Abstract

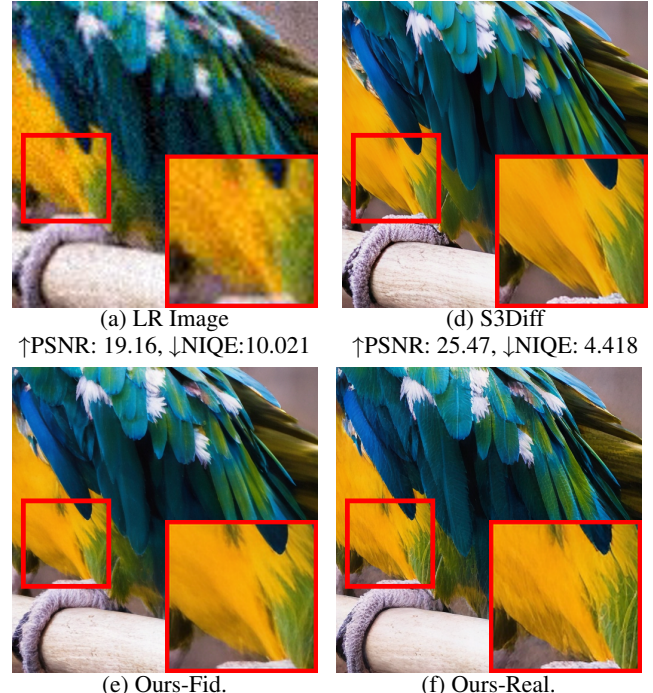
Pre-trained diffusion models have shown great potential in real-world image super-resolution (Real-ISR) tasks by enabling high-resolution reconstructions. While one-step diffusion (OSD) methods significantly improve efficiency compared to traditional multi-step approaches, they still have limitations in balancing fidelity and realism across diverse scenarios. Since the OSDs for SR are usually trained or distilled by a single timestep, they lack flexible control mechanisms to adaptively prioritize these competing objectives, which are inherently manageable in multi-step methods through adjusting sampling steps. To address this challenge, we propose a Realism Controlled One-step Diffusion (RCOD) framework for Real-ISR. RCOD provides a latent domain grouping strategy that enables explicit control over fidelity-realism trade-offs during the noise prediction phase with minimal training paradigm modifications and original training data. A degradation-aware sampling strategy is also introduced to align distillation regularization with the grouping strategy and enhance the controlling of trade-offs. Moreover, a visual prompt injection module is used to replace conventional text prompts with degradation-aware visual tokens, enhancing both restoration accuracy and semantic consistency. Our method achieves superior fidelity and perceptual quality while maintaining computational efficiency. Extensive experiments demonstrate that RCOD outperforms state-of-the-art OSD methods in both quantitative metrics and visual qualities, with flexible realism control capabilities in the inference stage. The code will be released.

Introduction

Image super-resolution (SR) (Dong et al. 2015c; Zhang et al. 2018d, 2021b; Ledig et al. 2017; Liang et al. 2021) aims to recover a high-resolution (HR) image from its low-resolution (LR) counterpart.

Traditional image super-resolution simplifies the degradation process as known noise, blur, or downsampling. In recent years, real-world image super-resolution (Real-ISR) (Zhang et al. 2021b; Wang et al. 2021c) has attracted more attention due to the increasing demand for reconstructing high-resolution images under real-world unknown degradations, which is more challenging and practical in real applications.

Copyright © 2026, Association for the Advancement of Artificial Intelligence (www.aaai.org). All rights reserved.



↑PSNR: 19.16, ↓NIQE: 10.021 ↑PSNR: 25.47, ↓NIQE: 4.418
 ↑PSNR: **26.94**, ↓NIQE: 4.049 ↑PSNR: 25.66, ↓NIQE: **3.913**
 Figure 1: While previous one-step diffusion methods, such as S3Diff (Zhang et al. 2024b) only yield one optimal result (b), our approach offers the flexibility to control images (c-d) with different fidelity-realism trade-offs during inference, enhancing practical applicability across different scenarios.

While recent advances in Stable Diffusion (SD) models (Ho, Jain, and Abbeel 2020; Song et al. 2020), especially the large-scale pretrained text-to-image (T2I) models have demonstrated unprecedented capabilities in various downstream vision tasks (Zhang, Rao, and Agrawala 2023; Rombach et al. 2022a). Some works leveraging pre-trained SD models for multi-step SR, such as DiffBIR (Lin et al. 2023c), StableSR (Wang et al. 2024a), and SeeSR (Wu et al. 2024b), have achieved remarkable SR quality through iterative latent space optimization. Though these methods achieve impressive perceptual quality, they suffer from computational inefficiency. The caused latency by multi-step sampling makes real-time applications impractical.

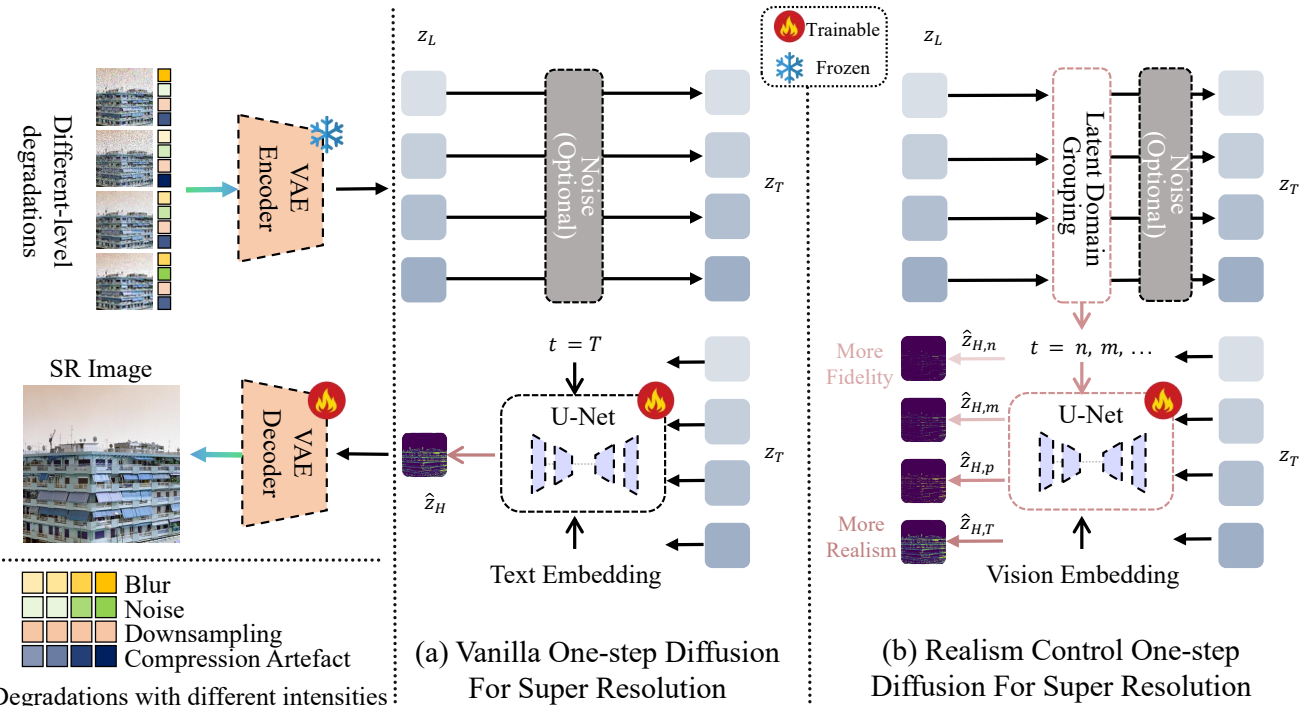


Figure 2: Realism control one-step diffusion (RCOD) training process. The left part illustrates several synthesized real-world LR images by applying diverse degradations with varying types and intensities on an HR image. (a) Existing vanilla one-step diffusion (OSD) methods for super-resolution (SR): These LR images are directly sent into the diffusion forward and reverse process; the denoising U-Net tends to learn to recover the ‘average’ degradation, leading to a monotonous generation ability within the latent domain. (b) Our proposed Realism Control One-Step Diffusion employs a latent domain grouping strategy. This allows for adaptive control of timesteps (denoising degrees) during the forward process according to the degradation degree in the latent domain. As a result, the denoising U-Net can acquire a more diverse generation capability based on the timestep.

To address the efficiency concerns, recent attempts focus on one-step diffusion frameworks (Wu et al. 2024a; Zhang et al. 2024b), which distill multi-step diffusion priors into single-step inference through knowledge distillation and achieve 10x to 100x speedup over previous multi-step diffusion-based SR methods. However, existing one-step diffusion approaches face a fundamental dilemma: the deterministic single-step generation inherently lacks the controllable fidelity-realism balance that multi-step methods achieve via step-wise noise scheduling. As illustrated in Fig. 1, previous one-step diffusion super-resolution (SR) methods, such as S3Diff (Zhang et al. 2024b), can only generate a single optimal result but can not meet the need for dynamic adjustment between fidelity and realism. The root cause lies in current OSD training paradigms. Most methods align all the LR inputs under different unknown degradations with a single convergence space through single timestep conditioned training, which results in a balanced static preference for fidelity or realism and prevents adaptive adjustments for scenario-specific requirements.

Bearing the above concerns in mind, we propose a novel framework that provides one-step diffusion Real-ISR methods with the capability to monotonically control the level of realism. This framework, which we denote as **Realism Controlled One-step Diffusion (RCOD)**, can be easily in-

tegrated into existing one-step diffusion methods for Real-ISR. Specifically, during the training phase, we incorporate a Latent Domain Grouping (LDG) strategy into the latent diffusion process, grouping training data according to a latent domain metric. Through this strategy, the diffusion denoising network learns to perceive variations in degradation across training samples, thereby gaining adaptive restoration capabilities. Furthermore, to address the inherent limitations caused by text prompts, we introduce a Visual Prompt Injection Module (VPIM) to enhance prompt quality. Our contributions are summarized as follows:

- We propose a simple but effective latent domain grouping (LDG) strategy that reformulates the noise prediction process by partitioning the latent space into fidelity-oriented and realism-oriented domains. This allows explicit control over detail preservation versus generative enhancement through simple training paradigm modifications, without requiring additional trainable parameters.
- During distillation, we introduce a degradation-aware sampling (DAS) strategy that reformulates timestep sampling in the pretrained model by adaptively aligning it with our LDG framework, enhancing controlling with regularization strength.
- To reduce the computational burden of VLM and de-

pendencies on manual text prompts, we propose a visual prompt injection module (VPIM) to replace text prompts with degradation-aware visual tokens, enhancing both restoration accuracy and semantic consistency.

- We empirically evaluate our approach on widely used stable diffusion-based and their distillation version Real-ISR methods, demonstrating quality improvement and the effectiveness of proposed approach.

Related Work

Real-World Image Super-Resolution

To address the challenge of recovering real-world low-resolution (LR) observations with unknown degradations, the Real-ISR task has been introduced. Due to the complex degradations involved, Real-ISR has been a challenging problem for some time (Ignatov et al. 2017; Liu et al. 2022a; Ji et al. 2020). Initial methods trained their models with simple downsampling techniques (Kim, Kwon Lee, and Mu Lee 2016a; Zhang et al. 2018d), which led to poor performance on real-world datasets. BSRGAN (Zhang et al. 2021b) and Real-ESRGAN (Wang et al. 2021c) were among the first to introduce a more realistic synthesis pipeline for LR images, enabling deep learning methods to be applied to real-world scenarios. However, these GAN-based methods often suffer from artifacts and training instability. With the emergence of the powerful pre-trained text-to-image generation model Stable Diffusion (SD) (Rombach et al. 2022a), many efforts have been made to leverage its strong generative capabilities for solving the Real-ISR problem, such as DiffBIR (Lin et al. 2023c), StableSR (Wang et al. 2024a) and SeeSR (Wu et al. 2024b), and FaithDiff (Chen, Pan, and Dong 2025). These SD-based methods improve fidelity and perceptual quality, but their application is limited due to the significant computational resources and time required. This is primarily due to the dozens to hundreds of timesteps involved in the diffusion denoising process.

One-step Diffusion Models for Real-ISR

To reduce the computational cost during inference, one-step diffusion methods have been proposed. These methods utilize model distillation techniques specifically designed for diffusion models, including progressive distillation (Meng et al. 2023; Salimans and Ho 2022), consistency models (Song et al. 2023), distribution matching distillation (Yin et al. 2024b,a), and variational score distillation (VSD) (Wang et al. 2024c; Nguyen and Tran 2024). In the context of Real-ISR, OSEDiff (Wu et al. 2024a) employs the VSD strategy to achieve one-step diffusion based on a pre-trained SD model. Similarly, S3Diff (Zhang et al. 2024b) directly employs a distilled Stable Diffusion Turbo (SD-T) model for Real-ISR. Recent works including ADCSR (Chen et al. 2025) and TSD-SR (Dong et al. 2025) also improve OSD performance and efficiency. InvSR(Yue, Liao, and Loy 2025) offers a flexible sampling mechanism with arbitrary-steps (1-5) diffusion.

However, while time efficiency is improved, another dilemma arises: one-step diffusion methods struggle to generate diverse outputs balancing fidelity and realism—a crit-

ical requirement for real-world applications—unlike multi-step approaches that achieve this through progressive noise scheduling. In other words, current one-step diffusion methods for Real-ISR cannot control fidelity and realism as effectively as their multi-step counterparts. Some techniques, such as ControlNet models (Zhang, Rao, and Agrawala 2023), can enhance HR image generation by controlling semantic content but cannot achieve pixel-level control and require additional conditions, such as extra images or depth maps. Therefore, these techniques cannot be directly employed in one-step diffusion methods for Real-ISR. PiSA-SR (Sun et al. 2025) controls fidelity and realism by training and inference with two different LoRA (Hu et al. 2022) modules within the U-Net and two-step diffusion, which obviously increases the computational cost compared to using a single step. Thus, a simple, efficient, and generalizable method for fidelity-realism control in OSD for Real-ISR remains essential.

Methodology

In this section, we first reveal the characteristic of denoising network in one-step diffusion for image super-resolution, and then propose our algorithm.

Preliminary: The Character of Denoising Network in One-step Diffusion for Real-ISR

In SD, the latent diffusion process starts with encoding an image into a latent representation \mathbf{z}_0 using a VAE encoder. The forward diffusion process then adds Gaussian noise to \mathbf{z}_0 over T steps via a Markov chain defined as:

$$q(\mathbf{z}_t | \mathbf{z}_{t-1}) = \mathcal{N}(\mathbf{z}_t; \sqrt{1 - \beta_t} \mathbf{z}_{t-1}, \beta_t \mathcal{I}) \quad (1)$$

following a variance schedule β_1, \dots, β_T . Here $\mathbf{z}_0 \sim q(\mathbf{z}_0)$. The forward process is: $\mathbf{z}_t = \alpha_t \mathbf{z}_0 + \sigma_t \epsilon$, where $\alpha_t = \prod_{s=1}^t \sqrt{1 - \beta_s}$, $\sigma_t = \sqrt{1 - \alpha_t^2}$, and $\epsilon \sim \mathcal{N}(\mathbf{0}, \mathcal{I})$. Here, the mean of \mathbf{z}_t becomes $\alpha_t \mathbf{z}_0$, and the variance is $\sigma_t^2 \mathcal{I}$. With larger t , more noise is added, resulting in a greater deviation of the mean (scaled by $\alpha_t < 1$) and an increased variance (σ_t^2), distancing \mathbf{z}_t from the original distribution \mathbf{z}_0 .

The reverse process denoises \mathbf{z}_t to recover \mathbf{z}_{t-1} :

$$p_\theta(\mathbf{z}_{t-1} | \mathbf{z}_t) = \mathcal{N}(\mathbf{z}_{t-1}; \boldsymbol{\mu}_\theta(\mathbf{z}_t, t), \boldsymbol{\Sigma}_\theta(\mathbf{z}_t, t)), \quad (2)$$

where a time-conditional U-Net ϵ_θ predicts the noise ϵ to estimate $\boldsymbol{\mu}_\theta$ and $\boldsymbol{\Sigma}_\theta$. Multi-step diffusion models iteratively refine \mathbf{z}_T back to \mathbf{z}_0 over T steps, while one-step diffusion methods, often distilled from multi-step models, predict the clean data directly from \mathbf{z}_T in a single step, significantly reducing computation.

For Real-ISR tasks using SD-based OSD methods like (Wu et al. 2024a), the process from LR latent features \mathbf{z}_L to HR latent features $\hat{\mathbf{z}}_H$ is formulated as a one-step denoising process:

$$\hat{\mathbf{z}}_H = F_\theta(\mathbf{z}_L; T, c_y) \triangleq \frac{\mathbf{z}_L - \beta_T \epsilon_\theta(\mathbf{z}_L; T, c_y)}{\alpha_T}, \quad (3)$$

where \mathbf{z}_L is the LR latent representation, c_y is the text embedding, and ϵ_θ is the denoising network predicting noise

at timestep T . As shown in Fig. 2(a), vanilla OSD methods learn a direct latent feature mapping from LR to HR images with or without adding additional noise.

In Real-ISR, images exhibit diverse degradation types and levels. SD-based methods use powerful generative image priors to recover LR images. However, OSD typically trains on all data with a fixed timestep T with a constant noise level. This results in a model that generates a uniform amount of detail and converges to a confined domain, which may not suit images with varying degradation severity. Tab. 1 (a) demonstrates the results of training OSEDiff on two different degradation pipelines (DP). ‘Orig.+ New Deg.’ denotes a DP applying more degradations than the standard DP (‘Orig.’). It indicates that higher degradation in training results in a greater emphasis on realism. This exposes OSD’s flaw: by locking training to a single fixed T , the model optimizes for an “**average**” **degradation**, yielding a limited generation flexibility that struggles to adapt its output to meet the specific scenario requirements.

In contrast, multi-step diffusion models provide greater flexibility in SR tasks. By selecting different timesteps t during the inference stage, these models control the degree of noise adding and removing in diffusion, balancing fidelity and realism effectively.

Therefore, to overcome the inherent limitation of OSD, which is incapable of adjusting its generation levels to adapt to varying scenarios, we propose a novel training strategy for real-world SR applications that can flexibly control the generation realism during the inference stage.

Metrics	Orig.	Orig.+New Deg.	M_L	L1	MSE	Cosine Sim.
PSNR \uparrow	25.15	24.59	SSIM \uparrow	0.60	0.54	0.78
MANIQA \uparrow	0.6326	0.6462	DISTS \uparrow	0.15	0.11	0.42
			CLIPQA \uparrow	0.06	0.05	0.27

(a)

(b)

Table 1: (a) Influence of degradation degree in training data. (b) |Spearman coefficient| \uparrow comparison of different M_L distances and image quality metrics.

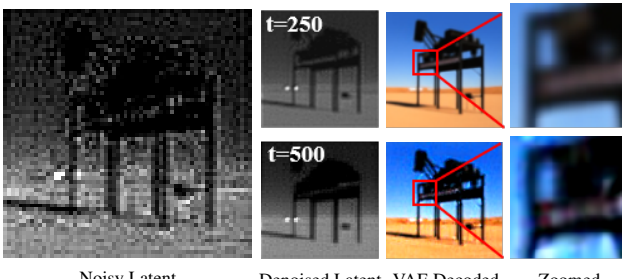


Figure 3: Influence of different timesteps t using SD-turbo.

Latent Domain Grouping

To achieve dynamic fidelity-realism trade-offs control in OSD generated SR results, we focus on the most basic condition in denoising network, *i.e.*, timestep condition. Unlike prompts from a text encoder or a vision encoder, the timestep condition is an unremovable component in the diffusion process. At the same time, it controls the mean and variance of noisy latent feature z_T . With the larger mean and variance difference between z_T and z_0 , more contents will be generated during the denoising process. Fig. 3 shows an example

of influence of different t . In the foundational model SD-turbo, the higher timestep value during the diffusion process usually reflects the the higher capability generating.

Therefore, to easily control the generation degree, we propose a latent domain grouping (LDG) strategy. Recall Eq. (3), we do not use a single fixed timestep T , but choose a timestep t according to a metrics:

$$\hat{z}_H = F_\theta(z_L; t, c_y), \quad (4)$$

$$t = k \cdot (n - \left\lfloor \frac{n \cdot (M_L - M_{L-\min})}{(M_{L-\max} - M_{L-\min})} \right\rfloor), \quad k \in \mathbb{Z}^+, \quad (5)$$

where M_L denotes a latent metric that can perceive the “level of degradation” of features in latent domain, $M_{L-\min}$ is the minimum value of M_L in training data, k is interval of timestep, $\lfloor \cdot \rfloor$ denotes the maximum integer no larger than the entry inside, n is number of groups for timestep.

To employ this strategy both on SD and distillation version of SD, *i.e.*, SD-Turbo (SDT), which distilled a four specific steps from the original 1000-step diffusion process, we set n to be ≤ 4 and $k = 250$.

By the grouping strategy, denoising network can learn different degrees of generation according to timestep. In the training stage, grouping is based on the M_L described in the next subsection. In the inference stage, we can easily choose a timestep to control the level of realism for SR in different scenarios. Furthermore, due to our grouping strategy, the realism level increases monotonically with the timestep.

Latent Metric for Denoising Network

The latent metric M_L is designed to enable the denoising network in the latent domain to perceive the “level of degradation” of the low-resolution features z_L . Here, we define the “level of degradation” as the extent to which z_L deviates from its HR counterpart z_H . Thus, the definition of the latent metric M_L should reflect the characteristics of z_L that indicate this degradation.

A simple choice might be to use the difference between the mean values of z_L and z_H , as the forward diffusion process scales the mean of z_L over time. However, as shown in Fig. 4(a), the mean values of z_L and z_H are similar across the training data. This suggests that mean difference fails to effectively capture the degradation level.

Instead, we use cosine similarity (CS) as M_L :

$$M_L = \frac{\mathbf{z}_L \cdot \mathbf{z}_H}{\|\mathbf{z}_L\| \|\mathbf{z}_H\|}. \quad (6)$$

Cosine similarity is a widely adopted measure in representation learning (e.g., contrastive learning (Chen et al. 2020)). It can quantify the divergence between high-dimensional latent features z_L and z_H , which can reflect high-level changes caused by degradation. As shown in Fig. 4(b), most cosine similarity values lie between 0 and 1, providing a clear range to distinguish varying degrees of degradation for the denoising network.

Different distances inherently introduce a certain preference or bias, to evaluate the bias of different M_L , we calculate correlation coefficient (|Spearman Corr.| \uparrow) of CS, L1,

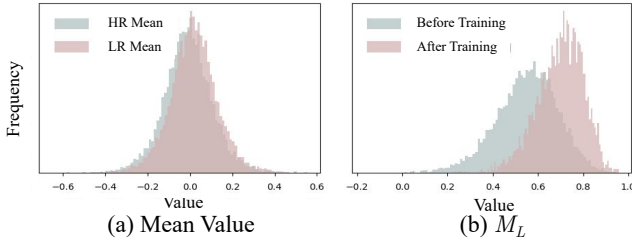


Figure 4: Distribution of (a) mean value of LR and HR training images in the latent domain, (b) the M_L metric in the latent domain of VAE before and after training.

and MSE with different metrics in Table 1 (b). The metrics are calculated between LR and HR images. The correlation reflects the degree of association between various M_L and different metrics. CS exhibits a higher correlation coefficient with objective (SSIM), perceptual (DISTTS), and semantic (CLIPQA) metrics compared to other distances in latent space. **More visualization results can be seen in Supplementary Materials (SM).**

Metric Estimation

Since \mathbf{z}_H is introduced as a latent metric, we can only calculate it during training. In the inference stage, beyond manually choosing a timestep, we also consider an adaptive timestep selection, i.e., estimating an M_L for each LR image. Benefiting from the powerful representation ability of the pre-trained model, we use features from intermediate layers as input and a simple MLP as a metric estimation module (MEM), operating independently of OSD training.

Degradation-aware Sampling Distillation

Previous VSD method for SR (Wu et al. 2024a), utilizes the regularization network (a pre-trained SD) that sampled timesteps across a wide range (20-980). This aims to generate regularization latent features and, in turn, optimize the distribution of the OSD network. However, to better integrate the distillation process with the concept of degradation in the latent space, we propose a Degradation-Aware Sampling (DAS) strategy. DAS redefines how timesteps are sampled in the pre-trained model, adaptively aligning this process with our LDG framework to provide explicit control over regularization strength. The DAS can be written as:

$$t_r = S(\max(20, t - k), \min(980, t + k)) \quad (7)$$

where t_r is the sample timestep for regularization network, t is the chosen timestep in OSD network by LDG, $S(t_{\min}, t_{\max})$ denotes uniformly random sampling of an integer from the range $[t_{\min}, t_{\max}]$.

By applying DAS, the degradation grouping information is delivered from LDG, thereby aligning this process with LDG and control over regularization strength.

Visual Prompt Injection Module

In previous SD-based super-resolution (SR) methods like OSEDiff (Wu et al. 2024a) and SeeSR (Wu et al. 2024b), text encoders, sometimes paired with a vision-language model (VLM) as a text prompt extractor, improve non-reference

(NR) metrics, which assess realism, but often constrain full-reference (FR) metrics, which assess fidelity to the ground truth. This trade-off arises because text prompts provide high-level semantic guidance to enhance realism, yet they may compromise structural accuracy.

LR feature \mathbf{z}_L solely from the VAE encoder offers limited semantic information. Without additional context, the conditioned U-Net struggles to generate high-quality outputs. Text prompts attempt to bridge this gap by injecting external semantic cues, but they come with drawbacks: VLMs increase computational costs, and the prompts may not fully align with the image’s content. Some methods like S3Diff (Zhang et al. 2024b) use fixed text to reduce complexity, yet still struggle to balance NR and FR metrics.

To address these issues, we propose the Visual Prompt Injection Module (VPIM), which replaces conventional text prompts with degradation-aware visual tokens. VPIM substitutes the text encoder (typically a CLIP text model) with a CLIP vision model and an MLP layer for dimension alignment. The LR image serves as its input, *i.e.*, visual prompt, and the output is fed into the cross-attention of the U-Net. By adopting VPIM, we eliminate the need for VLMs, reduce computational overhead, and provide the U-Net with image-specific semantic information directly from the LR input. The visual prompt is tied to the image’s pixel characteristics, leading to improvement in both fidelity and realism.

With the combination of LDG, latent metric, DAS, and VPIM, we proposed a Realism control one-step diffusion (RCOD) framework, a realism-flexible one-step diffusion model with enhanced performance that can be applied to various recent mainstream one-step diffusion Real-ISR methods, thereby improving their capabilities. **We provide a pseudo-code example of our RCOD in SM.**

Experiments

Experiments Setups

Datasets: Following the training and testing settings of prior works(Wu et al. 2024b,a; Zhang et al. 2024b), we employ LSDIR (Li et al. 2023d) and the first 10K face images from FFHQ (Karras, Laine, and Aila 2019) for training and degradation pipeline of Real-ESRGAN (Wang et al. 2021c) for LR image synthesizing. The synthetic test data use cropped 512×512 synthetic data from DIV2K-Val (Agustsson and Timofte 2017) and degraded using the Real-ESRGAN pipeline (Wang et al. 2021c). The real-world data include LR-HR pairs from RealSR (Cai et al. 2019a) and DRealSR (Wei et al. 2020a), both with sizes of 128×128 - 512×512 for LR-HR pairs.

Evaluation Metrics: We employ widely used FR and NR metrics. FR metrics include PSNR, SSIM (Wang et al. 2004a), LPIPS (Zhang et al. 2018a), and DISTTS (Ding et al. 2020a). NR metrics include NIQE (Zhang, Zhang, and Bovik 2015a), MANIQA-pipal (Yang et al. 2022b), MUSIQ (Ke et al. 2021a), and CLIPQA (Wang, Chan, and Loy 2023a).

Method Comparison: We compare our method with state-of-the-art methods (SOTA) in three categories: multi-step diffusion Real-ISR methods, including StableSR (Wang

Datasets	Methods	PSNR↑	SSIM↑	LPIPS↓	DISTS↓	NIQE↓	MUSIQ↑	MANIQA↑	CLIPQA↑
DrealSR	SinSR	28.36	0.7515	0.3665	0.2485	6.991	55.33	0.4884	0.6383
	PiSA-SR	28.31	0.7804	0.2960	0.2169	6.200	66.11	0.6156	0.6970
	TSD-SR	25.67	0.7132	0.3538	0.2459	5.991	65.99	0.6327	0.7137
	InvSR	28.33	0.7502	0.3678	0.2481	6.941	55.27	0.4900	0.6385
	OSEDiff	27.92	0.7835	0.2968	0.2165	6.490	64.65	0.5899	0.6963
	RCOD _O -Fid.	28.90	0.7906	0.2919	0.2186	6.817	66.72	0.6275	0.7023
	RCOD _O -Neu.	28.30	0.7775	0.3080	0.2306	6.469	68.03	0.6385	0.7179
	RCOD _O -Real.	27.59	0.7600	0.3389	0.2499	6.172	68.19	0.6295	0.7325
	S3Diff	27.54	0.7491	0.3109	0.2099	6.212	63.94	0.6134	0.7130
	RCOD _S -Fid.	28.09	0.7800	0.3002	0.2149	5.871	65.74	0.6174	0.6963
	RCOD _S -Neu.	27.48	0.7526	0.3256	0.2251	5.636	67.40	0.6339	0.7278
	RCOD _S -Real.	26.95	0.7190	0.3607	0.2414	5.448	67.58	0.6317	0.7478
	RCOD _S -Adap.	27.83	0.7661	0.3098	0.2181	5.768	66.32	0.6223	0.7110
RealSR	SinSR	26.28	0.7347	0.3188	0.2353	6.287	60.80	0.5385	0.6122
	PiSA-SR	25.50	0.7417	0.2672	0.2044	5.500	70.15	0.6560	0.6702
	TSD-SR	23.41	0.6886	0.2805	0.2183	5.093	70.77	0.6311	0.7193
	InvSR	24.13	0.7125	0.2871	0.2123	5.626	68.54	0.6619	0.6790
	OSEDiff	25.15	0.7341	0.2921	0.2128	5.648	69.09	0.6326	0.6693
	RCOD _O -Fid.	26.01	0.7427	0.2796	0.2103	5.911	70.25	0.6647	0.6866
	RCOD _O -Neu.	25.39	0.7264	0.2939	0.2190	5.497	70.34	0.6750	0.7022
	RCOD _O -Real.	24.62	0.7011	0.3296	0.2375	5.341	70.76	0.6650	0.7084
	S3Diff	25.18	0.7269	0.2721	0.2005	5.269	67.82	0.6437	0.6727
	RCOD _S -Fid.	25.42	0.7392	0.2647	0.1976	5.095	69.46	0.6605	0.6509
	RCOD _S -Neu.	24.78	0.7130	0.2855	0.2073	5.024	70.55	0.6757	0.6886
	RCOD _S -Real.	24.08	0.6759	0.3228	0.2236	4.900	70.65	0.6719	0.7086
	RCOD _S -Adap.	25.23	0.7313	0.2714	0.2010	5.033	69.72	0.6646	0.6622

Table 2: Quantitative comparison with state-of-the-art methods on both synthetic and real-world benchmarks. The best and second best results within both multi-step and one-step diffusion-based methods are highlighted in red and blue, respectively.

et al. 2024a), ResShift (?), DiffBIR (Lin et al. 2023c), and SeeSR (Wu et al. 2024b); one-step diffusion Real-ISR methods, such as SinSR (Wang et al. 2024b), OSEDiff (Wu et al. 2024a), S3Diff (Zhang et al. 2024b), TSD-SR (Dong et al. 2025), PiSA-SR (default version) (Sun et al. 2025), and InvSR (Yue, Liao, and Loy 2025); and GAN-based methods, including BSRGAN (Zhang et al. 2021b) and Real-ESRGAN (Wang et al. 2021c). We quantitatively compare recent SOTA OSD methods in Table 2 on real-world data. **More qualitative comparisons and the full table including synthetic data, multi-step diffusion, and GAN-based methods are in SM.**

Implement Details

Model Setting: To verify our framework, we select two types of recent SOTA OSD Real-ISR methods: OSEDiff (Wu et al. 2024a), which is distilled from a pre-trained multi-step Stable Diffusion (SD) model, and S3Diff (Zhang et al. 2024b), which directly uses SD-T (a distilled version of SD), as our base models. When RCOD is applied to them, they are named RCOD_O and RCOD_S, respectively. The choice of $n = 3$ corresponds to three distinct generation levels in the inference stage: Fidelity, Neutral, and Realism. *i.e.*, $t = 250, 500$, and 750 during inference. Since the S3Diff is not directly distilled from a multi-step diffusion, we do not apply DAS on it. RCOD_S-Adap. employs

MEM during inference. The input to the MEM in this case is z_L and the features in the last layer degradation estimation model used in (Zhang et al. 2024b). The MEM is trained after RCOD_S training, utilizing the same training data. **More details please refer to SM.**

Comparison with State-of-the-Arts

Quantitative Comparisons: We can observe in Table 2: *i*) By applying RCOD, on each dataset, the “-Fid.” versions ($t = 250$) have better full-reference (FR) metrics such as PSNR, SSIM, LPIPS, and FID, while keeping the no-reference (NR) metrics relatively ordinary. In contrast, the “-Real.” versions ($t = 750$) achieve obviously higher NR metrics like MANIQA, MUSIQ, and CLIPQA. Most “-Neu.” versions ($t = 500$) fall within the middle range of the previous two versions. This illustrates that we can effectively and simply control the realism level (usually measured by perceptual NR metrics) during the inference stage, and that the realism level increases monotonically with the timestep. *ii*) RCOD_S-Adap. has relatively balanced metrics between RCOD_S-Fid. and RCOD_S-Neu.. This indicates that most estimated M_L values are closer to 1 than to 0. This roughly matches the cosine similarity value distributions in Fig. 4 (b). *iii*) When applying RCOD, RCOD_O-Fid. and RCOD_S-Adap. perform better than their original methods (OSEDiff and S3Diff, respectively) on most metrics, including PSNR,

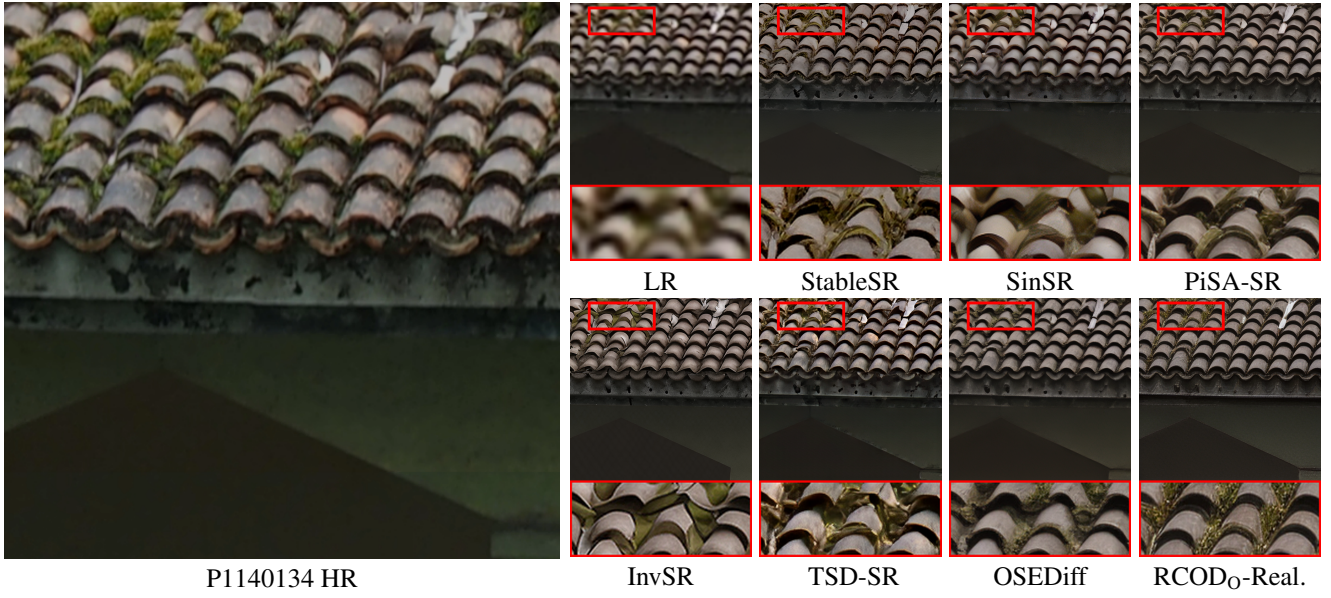


Figure 5: Visual comparison ($\times 4$) of $\text{RCOD}_\text{O-Real.}$ with other methods on DRealSR data.

SSIM, LPIPS, MANIQA, and MUSIQ. Even with a preference for fidelity in FR metrics, $\text{RCOD}_\text{O-Fid.}$ shows superior performance on some NR metrics, such as MANIQA and MUSIQ, compared to the original OSEDiff method on real-world data. Additionally, $\text{RCOD}_\text{S-Real.}$ usually achieves the best NR metrics (NIQE and CLIPQA). iv) S3Diff shows better performance on the perceptual quality metric DIST. This may arise from the negative online prompting (NOP) used in training, which provides a more accurate concept of high quality. However, since the text encoder and text prompt are replaced by VPIM in our RCOD_S , the NOP is also removed. Despite this, our $\text{RCOD}_\text{S-Adap.}$ performs better on other NR metrics.

Time Efficiency: In Table 3, we compare inference time and trainable parameters. All methods are tested on an A100 GPU with a 512×512 input image. RCOD keeps similar time efficiency and trainable parameters as the original methods while have higher PSNR and MANIQA. RCOD_O even inferences faster as the text extractor is removed.

Qualitative Comparisons: Fig. 5 compares the visual qualities of different Real-ISR methods. $\text{RCOD}_\text{O-Real.}$ demonstrates its ability to recover more detailed and natural textures. Fig. 6 illustrates the changes in visual effects as t increases, *i.e.*, from $\text{RCOD}_\text{S-Fid.}$ ($t = 250$) to $\text{RCOD}_\text{S-Real.}$ ($t = 750$). As t increases during the inference stage, more skin texture and wrinkles are recovered. $\text{RCOD}_\text{S-Adap.}$ chooses a proper $t = 500$ in this case, where the M_L range is $[0.5, 0.75]$ according to Eq. 5. The M_L of the LR image (0.621) falls within this range.

Ablation Study We performed a series of ablation studies of the RCOD framework, the details can be found in SM.

Conclusion

We propose RCOD , a framework that enhances one-step diffusion methods for Real-ISR through flexible realism



Figure 6: Visual comparison ($\times 4$) of realism controls during RCOD_S inference stage on DIV2K Validation dataset.

control. RCOD employs latent grouping with degradation-aware sampling during distillation and introduces a robust latent metric enabling denoising networks to assess degradation levels. Applied to two distinct one-step diffusion methods, RCOD achieves superior super-resolution performance across most FR and NR metrics while maintaining computational efficiency. We believe RCOD holds promise for diverse Real-ISR scenarios with varying requirements.

Metrics	PiSA-SR-adj.	OSEDiff	RCOD _{O-Fid.}	S3Diff	RCOD _{S-Adap.}
PSNR \uparrow	28.31	27.92	28.90	27.54	27.83
MANIQA \uparrow	0.6156	0.5899	0.6275	0.6134	0.6223
Infer. Time (s)	0.13	0.11	0.09	0.28	0.28
#Trainable Param. (M)	8.1	8.5	9.5	34.5	35.5

Table 3: Efficiency comparison on an NVIDIA A100 GPU. The best results are highlighted in bold.

References

- Abdelhamed, A.; Lin, S.; and Brown, M. S. 2018. A high-quality denoising dataset for smartphone cameras. In *CVPR*.
- Agustsson, E.; and Timofte, R. 2017. Ntire 2017 challenge on single image super-resolution: Dataset and study. In *CVPRW*, 126–135.
- Ahn, N.; Kang, B.; and Sohn, K.-A. 2018. Fast, accurate, and lightweight super-resolution with cascading residual network. In *ECCV*.
- Ali, A.; Touvron, H.; Caron, M.; Bojanowski, P.; Douze, M.; Joulin, A.; Laptev, I.; Neverova, N.; Synnaeve, G.; Verbeek, J.; et al. 2021. Xcit: Cross-covariance image transformers. In *NeurIPS*.
- An, J.; and Cho, S. 2015. Variational autoencoder based anomaly detection using reconstruction probability. *Special lecture on IE*, 2(1): 1–18.
- Arbelaez, P.; Maire, M.; Fowlkes, C.; and Malik, J. 2010. Contour detection and hierarchical image segmentation. *PAMI*.
- Ba, J. L.; Kiros, J. R.; and Hinton, G. E. 2016. Layer normalization. *arXiv preprint arXiv:1607.06450*.
- Bello, I.; Zoph, B.; Vaswani, A.; Shlens, J.; and Le, Q. V. 2019. Attention augmented convolutional networks. In *ICCV*.
- Bertasius, G.; Torresani, L.; Yu, S. X.; and Shi, J. 2017. Convolutional random walk networks for semantic image segmentation. In *CVPR*.
- Berthelot, D.; Autef, A.; Lin, J.; Yap, D. A.; Zhai, S.; Hu, S.; Zheng, D.; Talbott, W.; and Gu, E. 2023. Tract: Denoising diffusion models with transitive closure time-distillation. *arXiv preprint arXiv:2303.04248*.
- Bevilacqua, M.; Roumy, A.; Guillemot, C.; and Alberi-Morel, M. L. 2012. Low-complexity single-image super-resolution based on nonnegative neighbor embedding. In *BMVC*.
- Bishop, C. M. 2006. *Pattern recognition and machine learning*. Springer.
- Blalock, D.; Gonzalez, J. J.; Frankle, J.; and Guttag, J. V. 2020. What is the State of Neural Network Pruning? In *MLSys*.
- Bluche, T. 2016. Joint line segmentation and transcription for end-to-end handwritten paragraph recognition. In *NeurIPS*.
- Bo, L.; Ren, X.; and Fox, D. 2013. Multipath sparse coding using hierarchical matching pursuit. In *CVPR*.
- Breiman, L. 2001. Random forests. *Machine Learning*.
- Cai, J.; Zeng, H.; Yong, H.; Cao, Z.; and Zhang, L. 2019a. Toward real-world single image super-resolution: A new benchmark and a new model. In *ICCV*, 3086–3095.
- Cai, J.; Zeng, H.; Yong, H.; Cao, Z.; and Zhang, L. 2019b. Toward Real-World Single Image Super-Resolution: A New Benchmark and A New Model. *arXiv:1904.00523*.
- Cao, C.; Liu, X.; Yang, Y.; Yu, Y.; Wang, J.; Wang, Z.; Huang, Y.; Wang, L.; Huang, C.; Xu, W.; Ramanan, D.; and Huang, T. S. 2015. Look and think twice: Capturing top-down visual attention with feedback convolutional neural networks. In *ICCV*.
- Cao, J.; Li, Y.; Zhang, K.; and Van Gool, L. 2021. Video super-resolution transformer. *arXiv preprint arXiv:2106.06847*.
- Cao, Y.; Xu, J.; Lin, S.; Wei, F.; and Hu, H. 2019. Gcnet: Non-local networks meet squeeze-excitation networks and beyond. In *ICCVW*.
- Cao, Z.; Liu, X.; Gu, N.; Nahavandi, S.; Xu, D.; Zhou, C.; and Tan, M. 2016. A Fast Orientation Estimation Approach of Natural Images. *IEEE Trans. Syst., Man, Cybern., Syst.*, 46(11): 1589–1597.
- Caron, M.; Touvron, H.; Misra, I.; Jégou, H.; Mairal, J.; Bojanowski, P.; and Joulin, A. 2021. Emerging properties in self-supervised vision transformers. In *ICCV*, 9650–9660.
- Chakrabarti, A.; Rajagopalan, A.; and Chellappa, R. 2007. Super-resolution of face images using kernel PCA-based prior. *TMM*, 9(4): 888–892.
- Chan, K. C.; Zhou, S.; Xu, X.; and Loy, C. C. 2022. Investigating tradeoffs in real-world video super-resolution. In *CVPR*, 5962–5971.
- Chandra, S.; Usunier, N.; and Kokkinos, I. 2017. Dense and low-rank Gaussian CRFs using deep embeddings. In *ICCV*.
- Chang, H.; Yeung, D.-Y.; and Xiong, Y. 2004. Super-resolution through neighbor embedding. In *CVPR*.
- Charbonnier, P.; Blanc-Feraud, L.; Aubert, G.; and Barlaud, M. 1994. Two deterministic half-quadratic regularization algorithms for computed imaging. In *ICIP*.
- Chen, B.; Li, G.; Wu, R.; Zhang, X.; Chen, J.; Zhang, J.; and Zhang, L. 2025. Adversarial diffusion compression for real-world image super-resolution. In *CVPR*, 28208–28220.
- Chen, C.; Shi, X.; Qin, Y.; Li, X.; Han, X.; Yang, T.; and Guo, S. 2022a. Real-world blind super-resolution via feature matching with implicit high-resolution priors. In *ACM MM*.
- Chen, D.; Liang, J.; Zhang, X.; Liu, M.; Zeng, H.; and Zhang, L. 2023a. Human guided ground-truth generation for realistic image super-resolution. In *CVPR*, 14082–14091.
- Chen, H.; Gu, J.; and Zhang, Z. 2021. Attention in attention network for image super-resolution. *arXiv preprint arXiv:2104.09497*.
- Chen, H.; He, X.; Qing, L.; Wu, Y.; Ren, C.; Sheriff, R. E.; and Zhu, C. 2022b. Real-world single image super-resolution: A brief review. *Information Fusion*, 79: 124–145.
- Chen, H.; Wang, Y.; Guo, T.; Xu, C.; Deng, Y.; Liu, Z.; Ma, S.; Xu, C.; Xu, C.; and Gao, W. 2021a. Pre-trained image processing transformer. In *ICCV*.
- Chen, H.; Wang, Y.; Guo, T.; Xu, C.; Deng, Y.; Liu, Z.; Ma, S.; Xu, C.; Xu, C.; and Gao, W. 2021b. Pre-trained image processing transformer. In *CVPR*.
- Chen, J.; Pan, J.; and Dong, J. 2025. Faithdiff: Unleashing diffusion priors for faithful image super-resolution. In *CVPR*, 28188–28197.
- Chen, J.; Yu, J.; Ge, C.; Yao, L.; Xie, E.; Wu, Y.; Wang, Z.; Kwok, J.; Luo, P.; Lu, H.; et al. 2023b. PixArt- α : Fast Training of Diffusion Transformer for Photorealistic Text-to-Image Synthesis. *arXiv preprint arXiv:2310.00426*.
- Chen, R.; Panda, R.; and Fan, Q. 2022. RegionViT: Regional-to-Local Attention for Vision Transformers. In *ICLR*.
- Chen, T.; Kornblith, S.; Norouzi, M.; and Hinton, G. 2020. A simple framework for contrastive learning of visual representations. In *ICML*, 1597–1607.
- Chen, X.; Li, L.-J.; Fei-Fei, L.; and Gupta, A. 2018. Iterative visual reasoning beyond convolutions. In *CVPR*.
- Chen, X.; Wang, X.; Zhou, J.; and Dong, C. 2022c. Activating More Pixels in Image Super-Resolution Transformer. *arXiv preprint arXiv:2205.04437*.

- Chen, X.; Wang, X.; Zhou, J.; Qiao, Y.; and Dong, C. 2023c. Activating more pixels in image super-resolution transformer. In *CVPR*, 22367–22377.
- Chen, Y.; Rohrbach, M.; Yan, Z.; Shuicheng, Y.; Feng, J.; and Kalantidis, Y. 2019. Graph-based global reasoning networks. In *CVPR*.
- Chen, Z.; Zhang, Y.; Gu, J.; Kong, L.; Yang, X.; and Yu, F. 2023d. Dual Aggregation Transformer for Image Super-Resolution. In *ICCV*, 12312–12321.
- Chen, Z.; Zhang, Y.; Gu, J.; Kong, L.; Yang, X.; and Yu, F. 2023e. Dual Aggregation Transformer for Image Super-Resolution. In *ICCV*.
- Chen, Z.; Zhang, Y.; Gu, J.; Yuan, X.; Kong, L.; Chen, G.; and Yang, X. 2023f. Image Super-Resolution with Text Prompt Diffusion. *arXiv preprint arXiv:2311.14282*.
- Chen, Z.; Zhang, Y.; Gu, J.; Zhang, Y.; Kong, L.; and Yuan, X. 2022d. Cross Aggregation Transformer for Image Restoration. In *NeurIPS*.
- Cheng, C.; Fu, Y.; Jiang, Y.-G.; Liu, W.; Lu, W.; Feng, J.; and Xue, X. 2018a. Dual skipping networks. In *CVPR*.
- Cheng, J.; Wang, P.-s.; Li, G.; Hu, Q.-h.; and Lu, H.-q. 2018b. Recent advances in efficient computation of deep convolutional neural networks. *Frontiers of Information Technology & Electronic Engineering*, 19(1): 64–77.
- Cheng, S.; Wang, Y.; Huang, H.; Liu, D.; Fan, H.; and Liu, S. 2021. Nbnet: Noise basis learning for image denoising with subspace projection. In *CVPR*.
- Cheng, X.; Li, X.; Tai, Y.; and Yang, J. 2018c. SESR: Single Image Super Resolution with Recursive Squeeze and Excitation Networks. *arXiv preprint arXiv:1801.10319*.
- Cheng, Y.; Wang, D.; Zhou, P.; and Zhang, T. 2018d. Model compression and acceleration for deep neural networks: The principles, progress, and challenges. *IEEE Signal Processing Magazine*, 35(1): 126–136.
- Choi, J.-H.; Kim, J.-H.; Cheon, M.; and Lee, J.-S. 2018. Lightweight and Efficient Image Super-Resolution with Block State-based Recursive Network. *arXiv preprint arXiv:1811.12546*.
- Choi, J.-S.; and Kim, M. 2017. A deep convolutional neural network with selection units for super-resolution. In *CVPRW*.
- Chollet, F. 2017. Xception: Deep learning with depthwise separable convolutions. In *CVPR*.
- Chu, X.; Tian, Z.; Wang, Y.; Zhang, B.; Ren, H.; Wei, X.; Xia, H.; and Shen, C. 2021a. Twins: Revisiting the design of spatial attention in vision transformers. In *NeurIPS*.
- Chu, X.; Tian, Z.; Zhang, B.; Wang, X.; Wei, X.; Xia, H.; and Shen, C. 2021b. Conditional positional encodings for vision transformers. *arXiv preprint arXiv:2102.10882*.
- Chu, X.; Zhang, B.; Ma, H.; Xu, R.; and Li, Q. 2019a. Fast, accurate and lightweight super-resolution with neural architecture search. *arXiv preprint arXiv:1901.07261*.
- Chu, X.; Zhang, B.; Xu, R.; and Ma, H. 2019b. Multi-objective reinforced evolution in mobile neural architecture search. *arXiv preprint arXiv:1901.01074*.
- Chung, H.; Kim, J.; Mccann, M. T.; Klasky, M. L.; and Ye, J. C. 2022a. Diffusion Posterior Sampling for General Noisy Inverse Problems. In *ICLR*.
- Chung, H.; Sim, B.; Ryu, D.; and Ye, J. C. 2022b. Improving diffusion models for inverse problems using manifold constraints. In *NeurIPS*.
- Chung, H.; Sim, B.; and Ye, J. C. 2022. Come-closer-diffuse-faster: Accelerating conditional diffusion models for inverse problems through stochastic contraction. In *CVPR*.
- Cortes, C.; Mohri, M.; and Rostamizadeh, A. 2012. Algorithms for learning kernels based on centered alignment. *JMLR*.
- Cui, Z.; Chang, H.; Shan, S.; Zhong, B.; and Chen, X. 2014. Deep network cascade for image super-resolution. In *ECCV*.
- Dai, D.; Timofte, R.; and Van Gool, L. 2015. Jointly optimized regressors for image super-resolution. In *Eurographics*.
- Dai, J.; Qi, H.; Xiong, Y.; Li, Y.; Zhang, G.; Hu, H.; and Wei, Y. 2017. Deformable convolutional networks. In *ICCV*.
- Dai, T.; Cai, J.; Zhang, Y.; Xia, S.-T.; and Zhang, L. 2019a. Second-order attention network for single image super-resolution. In *CVPR*, 11065–11074.
- Dai, T.; Cai, J.; Zhang, Y.; Xia, S.-T.; and Zhang, L. 2019b. Second-order Attention Network for Single Image Super-Resolution. In *CVPR*.
- Dai, T.; Cai, J.; Zhang, Y.; Xia, S.-T.; and Zhang, L. 2019c. Second-order Attention Network for Single Image Super-Resolution. In *CVPR*.
- Darbon, J.; Cunha, A.; Chan, T. F.; Osher, S.; and Jensen, G. J. 2008. Fast nonlocal filtering applied to electron cryomicroscopy. In *Proc. 5th IEEE Symp. Biomed. Imag.*, 1331–1334.
- Delbracio, M.; and Milanfar, P. 2023. Inversion by Direct Iteration: An Alternative to Denoising Diffusion for Image Restoration. *Transactions on Machine Learning Research (TMLR)*.
- Dhariwal, P.; and Nichol, A. 2021. Diffusion models beat gans on image synthesis. *NeurIPS*, 34: 8780–8794.
- Ding, K.; Ma, K.; Wang, S.; and Simoncelli, E. P. 2020a. Image quality assessment: Unifying structure and texture similarity. *IEEE PAMI*, 44(5): 2567–2581.
- Ding, K.; Ma, K.; Wang, S.; and Simoncelli, E. P. 2020b. Image quality assessment: Unifying structure and texture similarity. *PAMI*.
- Ding, X.; Ding, G.; Guo, Y.; Han, J.; and Yan, C. 2019. Approximated Oracle Filter Pruning for Destructive CNN Width Optimization. In *ICML*.
- Ding, X.; Ding, G.; Han, J.; and Tang, S. 2018. Auto-balanced filter pruning for efficient convolutional neural networks. In *AAAI*.
- Dodgson, N. A. 1997. Quadratic interpolation for image resampling. *TIP*.
- Dong, C.; Deng, Y.; Change Loy, C.; and Tang, X. 2015a. Compression artifacts reduction by a deep convolutional network. In *IEEE Int. Conf. Comput. Vis.*, 576–584.
- Dong, C.; Deng, Y.; Loy, C. C.; and Tang, X. 2015b. Compression artifacts reduction by a deep convolutional network. In *ICCV*.
- Dong, C.; Loy, C. C.; He, K.; and Tang, X. 2014. Learning a deep convolutional network for image super-resolution. In *ECCV*, 184–199. Springer.
- Dong, C.; Loy, C. C.; He, K.; and Tang, X. 2015c. Image super-resolution using deep convolutional networks. *IEEE transactions on pattern analysis and machine intelligence*, 38(2): 295–307.
- Dong, C.; Loy, C. C.; He, K.; and Tang, X. 2016. Image super-resolution using deep convolutional networks. *PAMI*.
- Dong, C.; Loy, C. C.; and Tang, X. 2016. Accelerating the super-resolution convolutional neural network. In *ECCV*.
- Dong, L.; Fan, Q.; Guo, Y.; Wang, Z.; Zhang, Q.; Chen, J.; Luo, Y.; and Zou, C. 2025. Tsd-sr: One-step diffusion with target score distillation for real-world image super-resolution. In *CVPR*, 23174–23184.

- Dong, W.; Shi, G.; and Li, X. 2013. Nonlocal Image Restoration With Bilateral Variance Estimation: A Low-Rank Approach. *IEEE TIP*.
- Dong, W.; Zhang, L.; Lukac, R.; and Shi, G. 2013a. Sparse representation based image interpolation with nonlocal autoregressive modeling. *TIP*.
- Dong, W.; Zhang, L.; Shi, G.; and Li, X. 2012. Nonlocally centralized sparse representation for image restoration. *IEEE TIP*.
- Dong, W.; Zhang, L.; Shi, G.; and Li, X. 2013b. Nonlocally centralized sparse representation for image restoration. *TIP*.
- Dong, W.; Zhang, L.; Shi, G.; and Wu, X. 2011. Image deblurring and super-resolution by adaptive sparse domain selection and adaptive regularization. *TIP*.
- Dong, X.; Bao, J.; Chen, D.; Zhang, W.; Yu, N.; Yuan, L.; Chen, D.; and Guo, B. 2022. Cswin transformer: A general vision transformer backbone with cross-shaped windows. In *CVPR*.
- Donoho, D. L. 2006. Compressed sensing. *TIT*.
- Dosovitskiy, A.; Beyer, L.; Kolesnikov, A.; Weissenborn, D.; Zhai, X.; Unterthiner, T.; Dehghani, M.; Minderer, M.; Heigold, G.; Gelly, S.; et al. 2021. An image is worth 16x16 words: Transformers for image recognition at scale. In *ICLR*.
- Duffau, H.; Capelle, L.; Denvil, D.; Sicchez, N.; Gatignol, P.; Lopes, M.; Mitchell, M.; Sicchez, J.; and Van Effenterre, R. 2003. Functional recovery after surgical resection of low grade gliomas in eloquent brain: hypothesis of brain compensation. *Journal of Neurology, Neurosurgery & Psychiatry*, 74(7): 901–907.
- Dumoulin, V.; Shlens, J.; and Kudlur, M. 2017. A learned representation for artistic style. In *ICLR*.
- Elsken, T.; Metzen, J. H.; and Hutter, F. 2019. Neural Architecture Search: A Survey. *JMLR*.
- Esser, P.; Kulal, S.; Blattmann, A.; Entezari, R.; Müller, J.; Saini, H.; Levi, Y.; Lorenz, D.; Sauer, A.; Boesel, F.; et al. 2024. Scaling rectified flow transformers for high-resolution image synthesis. In *ICML*.
- Esser, P.; Rombach, R.; and Ommer, B. 2021. Taming transformers for high-resolution image synthesis. In *CVPR*.
- Fan, Y.; Shi, H.; Yu, J.; Liu, D.; Han, W.; Yu, H.; Wang, Z.; Wang, X.; and Huang, T. S. 2017. Balanced two-stage residual networks for image super-resolution. In *CVPRW*.
- Fan, Y.; Yu, J.; Mei, Y.; Zhang, Y.; Fu, Y.; Liu, D.; and Huang, T. S. 2020. Neural Sparse Representation for Image Restoration. In *NeurIPS*.
- Fei, B.; Lyu, Z.; Pan, L.; Zhang, J.; Yang, W.; Luo, T.; Zhang, B.; and Dai, B. 2023. Generative Diffusion Prior for Unified Image Restoration and Enhancement. In *CVPR*, 9935–9946.
- Fernandez-Granda, C.; and Candes, E. 2013. Super-resolution via transform-invariant group-sparse regularization. In *IEEE Int. Conf. Comput. Vis.*, 3336–3343.
- Foi, A.; Katkovnik, V.; and Egiazarian, K. 2007. Pointwise shape-adaptive DCT for high-quality denoising and deblocking of grayscale and color images. *TIP*.
- Fookes, C.; Lin, F.; Chandran, V.; and Sridharan, S. 2012. Evaluation of image resolution and super-resolution on face recognition performance. *Journal of Visual Communication and Image Representation*.
- Freeman, W. T.; Pasztor, E. C.; and Carmichael, O. T. 2000. Learning low-level vision. *IJCV*.
- Gale, T.; Elsen, E.; and Hooker, S. 2019. The state of sparsity in deep neural networks. *arXiv preprint arXiv:1902.09574*.
- Gandikota, K. V.; and Chandramouli, P. 2024. Text-guided Explorable Image Super-resolution. *arXiv preprint arXiv:2403.01124*.
- Gao, S.; Liu, X.; Zeng, B.; Xu, S.; Li, Y.; Luo, X.; Liu, J.; Zhen, X.; and Zhang, B. 2023. Implicit diffusion models for continuous super-resolution. In *CVPR*.
- Geng, Z.; Pokle, A.; and Kolter, J. Z. 2024. One-step diffusion distillation via deep equilibrium models. In *NeurIPS*.
- Gilbert, C. D.; and Li, W. 2013. Top-down influences on visual processing. *Nature Reviews Neuroscience*, 14(5): 350.
- Girshick, R. 2015. Fast R-CNN. In *ICCV*.
- Glasner, D.; Bagam, S.; and Irani, M. 2009. Super-resolution from a single image. In *ICCV*.
- Glorot, X.; Bordes, A.; and Bengio, Y. 2011. Deep sparse rectifier neural networks. In *AISTATS*.
- Goodfellow, I.; Pouget-Abadie, J.; Mirza, M.; Xu, B.; Warde-Farley, D.; Ozair, S.; Courville, A.; and Bengio, Y. 2014. Generative adversarial nets. In *NeurIPS*.
- Goodfellow, I.; Pouget-Abadie, J.; Mirza, M.; Xu, B.; Warde-Farley, D.; Ozair, S.; Courville, A.; and Bengio, Y. 2020a. Generative adversarial networks. *Communications of the ACM*, 63(11): 139–144.
- Goodfellow, I.; Pouget-Abadie, J.; Mirza, M.; Xu, B.; Warde-Farley, D.; Ozair, S.; Courville, A.; and Bengio, Y. 2020b. Generative adversarial networks. *COMMUN ACM*.
- Gu, J.; and Dong, C. 2021. Interpreting super-resolution networks with local attribution maps. In *CVPR*.
- Gu, J.; Zhao, H.; Lin, Z.; Li, S.; Cai, J.; and Ling, M. 2019a. Scene graph generation with external knowledge and image reconstruction. In *CVPR*.
- Gu, S.; Lugmayr, A.; Danelljan, M.; Fritzsche, M.; Lamour, J.; and Timofte, R. 2019b. Div8k: Diverse 8k resolution image dataset. In *ICCV Workshop*.
- Gu, S.; Zuo, W.; Xie, Q.; Meng, D.; Feng, X.; and Zhang, L. 2015. Convolutional sparse coding for image super-resolution. In *ICCV*.
- Guan, L. 1996. An optimal neuron evolution algorithm for constrained quadratic programming in image restoration. *IEEE Trans. Syst., Man, Cybern. A, Syst., Humans*.
- Gubin, L.; Polyak, B.; and Raik, E. 1967. The method of projections for finding the common point of convex sets. *USSR Comput. Math. Math. Phys.*, 7(6): 1–24.
- Guo, J.; Han, K.; Wu, H.; Tang, Y.; Chen, X.; Wang, Y.; and Xu, C. 2022. Cmt: Convolutional neural networks meet vision transformers. In *CVPR*.
- Guo, Y.; Chen, J.; Wang, J.; Chen, Q.; Cao, J.; Deng, Z.; Xu, Y.; and Tan, M. 2020. Closed-loop Matters: Dual Regression Networks for Single Image Super-Resolution. In *CVPR*.
- Ha, D.; Dai, A.; and Le, Q. V. 2016. Hypernetworks. *arXiv preprint arXiv:1609.09106*.
- Han, S.; Liu, X.; and Mao, H. 2016. EIE: efficient inference engine on compressed deep neural network. *ACM Sigarch Computer Architecture News*, 44(3): 243–254.
- Han, S.; Mao, H.; and Dally, W. J. 2016. Deep compression: Compressing deep neural networks with pruning, trained quantization and huffman coding. In *ICLR*.
- Han, S.; Pool, J.; Tran, J.; and Dally, W. J. 2015. Learning both weights and connections for efficient neural network. In *NeurIPS*.
- Haris, M.; Shakhnarovich, G.; and Ukita, N. 2018. Deep Back-Projection Networks For Super-Resolution. In *CVPR*.

- Harnad, S. 1990. The symbol grounding problem. *Physica D: Nonlinear Phenomena*.
- Hassibi, B.; and Stork, D. G. 1993. Second order derivatives for network pruning: Optimal brain surgeon. In *NeurIPS*.
- He, K.; Zhang, X.; Ren, S.; and Sun, J. 2016. Deep residual learning for image recognition. In *CVPR*, 770–778.
- He, L.; Qi, H.; and Zaretzki, R. 2013. Beta process joint dictionary learning for coupled feature spaces with application to single image super-resolution. In *CVPR*.
- He, X.; Mo, Z.; Wang, P.; Liu, Y.; Yang, M.; and Cheng, J. 2019. ODE-Inspired Network Design for Single Image Super-Resolution. In *CVPR*.
- He, Y.; Zhang, X.; and Sun, J. 2017. Channel pruning for accelerating very deep neural networks. In *ICCV*.
- He, Z.; Dai, T.; Lu, J.; Jiang, Y.; and Xia, S.-T. 2020. Fakd: Feature-Affinity Based Knowledge Distillation for Efficient Image Super-Resolution. In *ICIP*.
- Hendrycks, D.; Mu, N.; Cubuk, E. D.; Zoph, B.; Gilmer, J.; and Lakshminarayanan, B. 2019. Augmix: A simple data processing method to improve robustness and uncertainty. *arXiv preprint arXiv:1912.02781*.
- Hertz, A.; Mokady, R.; Tenenbaum, J.; Aberman, K.; Pritch, Y.; and Cohen-Or, D. 2022. Prompt-to-prompt image editing with cross attention control. *arXiv preprint arXiv:2208.01626*.
- Heusel, M.; Ramsauer, H.; Unterthiner, T.; Nessler, B.; and Hochreiter, S. 2017a. Gans trained by a two time-scale update rule converge to a local nash equilibrium. *NeurIPS*, 30.
- Heusel, M.; Ramsauer, H.; Unterthiner, T.; Nessler, B.; and Hochreiter, S. 2017b. Gans trained by a two time-scale update rule converge to a local nash equilibrium. *NeurIPS*, 30.
- Hinton, G.; Vinyals, O.; and Dean, J. 2014. Distilling the knowledge in a neural network. In *NeurIPS Workshop*.
- Hinton, G.; Vinyals, O.; and Dean, J. 2015. Distilling the knowledge in a neural network. *arXiv preprint arXiv:1503.02531*.
- Ho, J.; Jain, A.; and Abbeel, P. 2020. Denoising diffusion probabilistic models. In *NeurIPS*.
- Ho, J.; and Salimans, T. 2022. Classifier-free diffusion guidance. *arXiv preprint arXiv:2207.12598*.
- Hobbs, J. R.; Stickel, M. E.; and Martin, P. 1993. Interpretation as abduction. *Artificial intelligence*.
- Howard, A. G.; Zhu, M.; Chen, B.; Kalenichenko, D.; Wang, W.; Weyand, T.; Andreetto, M.; and Adam, H. 2017. Mobilenets: Efficient convolutional neural networks for mobile vision applications. *arXiv preprint arXiv:1704.04861*.
- Hu, E. J.; Shen, Y.; Wallis, P.; Allen-Zhu, Z.; Li, Y.; Wang, S.; Wang, L.; and Chen, W. 2022. Lora: Low-rank adaptation of large language models. In *ICLR*.
- Hu, J.; Shen, L.; and Sun, G. 2018. Squeeze-and-excitation networks. In *CVPR*.
- Huang, G.; Liu, Z.; Weinberger, K. Q.; and van der Maaten, L. 2017. Densely connected convolutional networks. In *CVPR*.
- Huang, J.-B.; Singh, A.; and Ahuja, N. 2015. Single Image Super-resolution from Transformed Self-Exemplars. In *CVPR*.
- Huang, Z.; Wang, X.; Huang, L.; Huang, C.; Wei, Y.; and Liu, W. 2019. Ccnet: Criss-cross attention for semantic segmentation. In *ICCV*.
- Hui, Z.; Gao, X.; Yang, Y.; and Wang, X. 2019. Lightweight image super-resolution with information multi-distillation network. In *ACM MM*.
- Ignatov, A.; Kobyshev, N.; Timofte, R.; Vanhoey, K.; and Van Gool, L. 2017. Dslr-quality photos on mobile devices with deep convolutional networks. In *ICCV*.
- inference framework, D. 2024. Accessed: 20, 05, 2024.
- Ioffe, S.; and Szegedy, C. 2015. Batch Normalization: Accelerating Deep Network Training by Reducing Internal Covariate Shift. In *ICML*.
- Irani, M.; and Peleg, S. 1993. Motion analysis for image enhancement: Resolution, occlusion, and transparency. *J. Vis. Commun. Image Represent.*
- Jaderberg, M.; Simonyan, K.; Zisserman, A.; and Kavukcuoglu, K. 2015. Spatial transformer networks. In *NeurIPS*.
- Jancsary, J.; Nowozin, S.; and Rother, C. 2012. Loss-specific training of non-parametric image restoration models: A new state of the art. In *ECCV*, 112–125. Springer.
- Jarzynski, C. 1997. Equilibrium free-energy differences from nonequilibrium measurements: A master-equation approach. *Physical Review E*, 56(5): 5018.
- Ji, X.; Cao, Y.; Tai, Y.; Wang, C.; Li, J.; and Huang, F. 2020. Real-world super-resolution via kernel estimation and noise injection. In *CVPRW*.
- Jia, X.; De Brabandere, B.; Tuytelaars, T.; and Gool, L. V. 2016. Dynamic filter networks. In *NeurIPS*.
- Jo, Y.; Wug Oh, S.; Kang, J.; and Joo Kim, S. 2018. Deep video super-resolution network using dynamic upsampling filters without explicit motion compensation. In *CVPR*.
- Johnson, J.; Alahi, A.; and Fei-Fei, L. 2016. Perceptual losses for real-time style transfer and super-resolution. In *ECCV*.
- Kang, L.-W.; Hsu, C.-C.; Zhuang, B.; Lin, C.-W.; and Yeh, C.-H. 2015. Learning-based joint super-resolution and deblocking for a highly compressed image. *TMM*, 17(7): 921–934.
- Kang, M.; and Han, B. 2020. Operation-Aware Soft Channel Pruning using Differentiable Masks. In *ICML*.
- Karras, T.; Aila, T.; Laine, S.; and Lehtinen, J. 2017. Progressive Growing of GANs for Improved Quality, Stability, and Variation. *submitted to ICLR 2018*.
- Karras, T.; Aittala, M.; Aila, T.; and Laine, S. 2022. Elucidating the design space of diffusion-based generative models. In *NeurIPS*.
- Karras, T.; Laine, S.; and Aila, T. 2019. A style-based generator architecture for generative adversarial networks. In *CVPR*.
- Karras, T.; Laine, S.; and Aila, T. 2024. A Style-Based Generator Architecture for Generative Adversarial Networks. In *CVPR*.
- Kawar, B.; Elad, M.; Ermon, S.; and Song, J. 2022. Denoising Diffusion Restoration Models. In *NeurIPS*.
- Ke, J.; Wang, Q.; Wang, Y.; Milanfar, P.; and Yang, F. 2021a. Musiq: Multi-scale image quality transformer. In *ICCV*.
- Ke, J.; Wang, Q.; Wang, Y.; Milanfar, P.; and Yang, F. 2021b. Musiq: Multi-scale image quality transformer. In *ICCV*.
- Keys, R. 1981. Cubic convolution interpolation for digital image processing. *IEEE Trans. Acoust., Speech, Signal Process.*
- Kim, J.; Kwon Lee, J.; and Mu Lee, K. 2016a. Accurate image super-resolution using very deep convolutional networks. In *CVPR*.
- Kim, J.; Kwon Lee, J.; and Mu Lee, K. 2016b. Deeply-Recursive Convolutional Network for Image Super-Resolution. In *CVPR*.
- Kim, K. I.; and Kwon, Y. 2010. Single-image super-resolution using sparse regression and natural image prior. *IEEE PAMI*.
- Kingma, D.; and Ba, J. 2015. Adam: A method for stochastic optimization. In *ICLR*.

- Kingma, D. P.; and Ba, J. 2014. Adam: A method for stochastic optimization. *arXiv preprint arXiv:1412.6980*.
- Kipf, T. N.; and Welling, M. 2017. Semi-Supervised Classification with Graph Convolutional Networks. In *ICLR*.
- Kong, X.; Liu, X.; Gu, J.; Qiao, Y.; and Dong, C. 2022. Reflash dropout in image super-resolution. In *CVPR*.
- Kong, X.; Zhao, H.; Qiao, Y.; and Dong, C. 2021. ClassSR: A General Framework to Accelerate Super-Resolution Networks by Data Characteristic. In *CVPR*.
- Kornblith, S.; Norouzi, M.; Lee, H.; and Hinton, G. 2019. Similarity of neural network representations revisited. In *NeurIPS*.
- Krishna, R.; Zhu, Y.; Groth, O.; Johnson, J.; Hata, K.; Kravitz, J.; Chen, S.; Kalantidis, Y.; Li, L.-J.; Shamma, D. A.; et al. 2017. Visual genome: Connecting language and vision using crowdsourced dense image annotations. *IJCV*.
- Kumari, N.; Zhang, R.; Shechtman, E.; and Zhu, J.-Y. 2022. Ensembling off-the-shelf models for gan training. In *CVPR*.
- Kusupati, A.; Ramanujan, V.; Somani, R.; Wortsman, M.; Jain, P.; Kakade, S.; and Farhadi, A. 2020. Soft Threshold Weight Reparameterization for Learnable Sparsity. In *ICML*.
- Kwon, Y.; Kim, K. I.; Tompkin, J.; Kim, J. H.; and Theobalt, C. 2015. Efficient learning of image super-resolution and compression artifact removal with semi-local Gaussian processes. *PAMI*.
- Lai, W.-S.; Huang, J.-B.; Ahuja, N.; and Yang, M.-H. 2017a. Deep Laplacian Pyramid Networks for Fast and Accurate Super-Resolution. In *CVPR*.
- Lai, W.-S.; Huang, J.-B.; Ahuja, N.; and Yang, M.-H. 2017b. Fast and Accurate Image Super-Resolution with Deep Laplacian Pyramid Networks. *arXiv:1710.01992*.
- Lao, N.; Mitchell, T.; and Cohen, W. W. 2011. Random walk inference and learning in a large scale knowledge base. In *EMNLP*.
- LeCun, Y.; Denker, J. S.; and Solla, S. A. 1990. Optimal brain damage. In *NeurIPS*.
- Ledig, C.; Theis, L.; Huszár, F.; Caballero, J.; Cunningham, A.; Acosta, A.; Aitken, A.; Tejani, A.; Totz, J.; Wang, Z.; et al. 2017. Photo-realistic single image super-resolution using a generative adversarial network. In *CVPR*, 4681–4690.
- Lee, C.-Y.; Xie, S.; Gallagher, P.; Zhang, Z.; and Tu, Z. 2015. Deeply-supervised nets. In *AISTATS*.
- Lee, W.; Lee, J.; Kim, D.; and Ham, B. 2020. Learning with privileged information for efficient image super-resolution. In *ECCV*.
- Li, H.; Kadav, A.; Durdanovic, I.; Samet, H.; and Graf, H. P. 2017. Pruning filters for efficient convnets. In *ICLR*.
- Li, H.; Yang, Y.; Chang, M.; Chen, S.; Feng, H.; Xu, Z.; Li, Q.; and Chen, Y. 2022a. SRDiff: Single image super-resolution with diffusion probabilistic models. *Neurocomputing*.
- Li, J.; Li, D.; Xiong, C.; and Hoi, S. 2022b. Blip: Bootstrapping language-image pre-training for unified vision-language understanding and generation. In *ICML*, 12888–12900. PMLR.
- Li, K.; Ding, Z.; Li, K.; Zhang, Y.; and Fu, Y. 2018a. Support neighbor loss for person re-identification. In *ACM Multimedia*.
- Li, K.; Kong, Y.; and Fu, Y. 2017. Multi-stream deep similarity learning networks for visual tracking. In *IJCAI*.
- Li, K.; Wu, Z.; Peng, K.-C.; Ernst, J.; and Fu, Y. 2018b. Tell Me Where to Look: Guided Attention Inference Network. In *CVPR*.
- Li, K.; Wu, Z.; Peng, K.-C.; Ernst, J.; and Fu, Y. 2019a. Guided attention inference network. *PAMI*.
- Li, K.; Zhang, Y.; Li, K.; Li, Y.; and Fu, Y. 2019b. Attention bridging network for knowledge transfer. In *ICCV*.
- Li, K.; Zhang, Y.; Li, K.; Li, Y.; and Fu, Y. 2019c. Visual semantic reasoning for image-text matching. In *ICCV*.
- Li, K.; Zhang, Y.; Li, K.; Li, Y.; and Fu, Y. 2019d. Visual semantic reasoning for image-text matching. In *ICCV*.
- Li, R.; Zhou, Q.; Guo, S.; Zhang, J.; Guo, J.; Jiang, X.; Shen, Y.; and Han, Z. 2023a. Dissecting arbitrary-scale super-resolution capability from pre-trained diffusion generative models. *arXiv preprint arXiv:2306.00714*.
- Li, W.; Piéch, V.; and Gilbert, C. D. 2004. Perceptual learning and top-down influences in primary visual cortex. *Nature neuroscience*, 7(6): 651–657.
- Li, W.; Zhang, D.; Liu, Z.; and Qiao, X. 2005. Fast block-based image restoration employing the improved best neighborhood matching approach. *IEEE Trans. Syst., Man, Cybern. A, Syst., Humans*, 35(4): 546–555.
- Li, X. 2005. Improved wavelet decoding via set theoretic estimation. *TCSVTs*, 15(1): 108–112.
- Li, X.; Liu, Y.; Lian, L.; Yang, H.; Dong, Z.; Kang, D.; Zhang, S.; and Keutzer, K. 2023b. Q-diffusion: Quantizing diffusion models. In *ICCV*, 17535–17545.
- Li, X.; and Orchard, M. T. 2001. New edge-directed interpolation. *TIP*.
- Li, Y.; Fan, Y.; Xiang, X.; Demandolx, D.; Ranjan, R.; Timofte, R.; and Van Gool, L. 2023c. Efficient and Explicit Modelling of Image Hierarchies for Image Restoration. In *CVPR*.
- Li, Y.; Zhang, K.; Liang, J.; Cao, J.; Liu, C.; Gong, R.; Zhang, Y.; Tang, H.; Liu, Y.; Demandolx, D.; et al. 2023d. Lsdir: A large scale dataset for image restoration. In *CVPR*, 1775–1787.
- Li, Z.; Liu, Y.; Chen, X.; Cai, H.; Gu, J.; Qiao, Y.; and Dong, C. 2022c. Blueprint Separable Residual Network for Efficient Image Super-Resolution. In *CVPR*.
- Li, Z.; Yang, J.; Liu, Z.; Yang, X.; Jeon, G.; and Wu, W. 2019e. Feedback Network for Image Super-Resolution. In *CVPR*.
- Li, Z.; Yang, J.; Liu, Z.; Yang, X.; Jeon, G.; and Wu, W. 2019f. Feedback Network for Image Super-Resolution. In *CVPR*.
- Liang, J.; Cao, J.; Sun, G.; Zhang, K.; Van Gool, L.; and Timofte, R. 2021. Swinir: Image restoration using swin transformer. In *ICCV*.
- Liang, J.; Zeng, H.; and Zhang, L. 2022a. Details or artifacts: A locally discriminative learning approach to realistic image super-resolution. In *CVPR*, 5657–5666.
- Liang, J.; Zeng, H.; and Zhang, L. 2022b. Efficient and degradation-adaptive network for real-world image super-resolution. In *ECCV*.
- Liew, A.-C.; and Yan, H. 2004. Blocking artifacts suppression in block-coded images using overcomplete wavelet representation. *TCSVT*, 14(4): 450–461.
- Lim, B.; Son, S.; Kim, H.; Nah, S.; and Lee, K. M. 2017a. Enhanced deep residual networks for single image super-resolution. In *CVPRW*.
- Lim, B.; Son, S.; Kim, H.; Nah, S.; and Mu Lee, K. 2017b. Enhanced deep residual networks for single image super-resolution. In *CVPRW*, 136–144.
- Lin, C.-H.; Gao, J.; Tang, L.; Takikawa, T.; Zeng, X.; Huang, X.; Kreis, K.; Fidler, S.; Liu, M.-Y.; and Lin, T.-Y. 2023a. Magic3d: High-resolution text-to-3d content creation. In *CVPR*, 300–309.
- Lin, S.; Liu, B.; Li, J.; and Yang, X. 2023b. Common Diffusion Noise Schedules and Sample Steps are Flawed. *arXiv preprint arXiv:2305.08891*.

- Lin, T.-Y.; Maire, M.; Belongie, S.; Hays, J.; Perona, P.; Ramanan, D.; Dollár, P.; and Zitnick, C. L. 2014. Microsoft coco: Common objects in context. In *ECCV*, 740–755. Springer.
- Lin, X.; He, J.; Chen, Z.; Lyu, Z.; Fei, B.; Dai, B.; Ouyang, W.; Qiao, Y.; and Dong, C. 2023c. Diffbir: Towards blind image restoration with generative diffusion prior. *arXiv preprint arXiv:2308.15070*.
- Lin, X.; Ma, L.; Liu, W.; and Chang, S.-F. 2020. Context-Gated Convolution. In *ECCV*.
- Lipman, Y.; Chen, R. T.; Ben-Hamu, H.; Nickel, M.; and Le, M. 2023. Flow Matching for Generative Modeling. In *ICLR*.
- List, P.; Joch, A.; Lainema, J.; Bjontegaard, G.; and Karczewicz, M. 2003. Adaptive deblocking filter. *TCSVT*, 13(7): 614–619.
- Liu, A.; Liu, Y.; Gu, J.; Qiao, Y.; and Dong, C. 2022a. Blind image super-resolution: A survey and beyond. *IEEE PAMI*, 45(5): 5461–5480.
- Liu, D.; Wen, B.; Fan, Y.; Loy, C. C.; and Huang, T. S. 2018. Non-local recurrent network for image restoration. In *NeurIPS*.
- Liu, H.; Li, C.; Wu, Q.; and Lee, Y. J. 2023a. Visual Instruction Tuning. In *NeurIPS*.
- Liu, H.; Li, C.; Wu, Q.; and Lee, Y. J. 2024. Visual instruction tuning. *NeurIPS*, 36.
- Liu, J.; Xu, Z.; Shi, R.; Cheung, R. C.; and So, H. K. 2020a. Dynamic Sparse Training: Find Efficient Sparse Network From Scratch With Trainable Masked Layers. In *ICLR*.
- Liu, J.; Zhang, W.; Tang, Y.; Tang, J.; and Wu, G. 2020b. Residual Feature Aggregation Network for Image Super-Resolution. In *CVPR*.
- Liu, J.; Zhang, W.; Tang, Y.; Tang, J.; and Wu, G. 2020c. Residual Feature Aggregation Network for Image Super-Resolution. In *CVPR*.
- Liu, K.; Jiang, Y.; Choi, I.; and Gu, J. 2023b. Learning Image-Adaptive Codebooks for Class-Agnostic Image Restoration. *arXiv preprint arXiv:2306.06513*.
- Liu, K.; Jiang, Y.; Choi, I.; and Gu, J. 2023c. Learning Image-Adaptive Codebooks for Class-Agnostic Image Restoration. *arXiv preprint arXiv:2306.06513*.
- Liu, L.; Ren, Y.; Lin, Z.; and Zhao, Z. 2022b. Pseudo numerical methods for diffusion models on manifolds. In *ICLR*.
- Liu, X.; Gong, C.; and Liu, Q. 2022. Flow straight and fast: Learning to generate and transfer data with rectified flow. *arXiv preprint arXiv:2209.03003*.
- Liu, X.; Zhang, X.; Ma, J.; Peng, J.; et al. 2023d. Instaflow: One step is enough for high-quality diffusion-based text-to-image generation. In *ICLR*.
- Liu, Z.; Li, J.; Shen, Z.; Huang, G.; Yan, S.; and Zhang, C. 2017. Learning efficient convolutional networks through network slimming. In *ICCV*.
- Liu, Z.; Lin, Y.; Cao, Y.; Hu, H.; Wei, Y.; Zhang, Z.; Lin, S.; and Guo, B. 2021. Swin transformer: Hierarchical vision transformer using shifted windows. In *ICCV*.
- Loshchilov, I.; and Hutter, F. 2017. Sgdr: Stochastic gradient descent with warm restarts. In *ICLR*.
- Loshchilov, I.; and Hutter, F. 2019. Decoupled weight decay regularization. In *ICLR*.
- Louizos, C.; Welling, M.; and Kingma, D. P. 2018. Learning Sparse Neural Networks through L_0 Regularization. In *ICLR*.
- Lu, C.; Zhou, Y.; Bao, F.; Chen, J.; Li, C.; and Zhu, J. 2022a. Dpm-solver: A fast ode solver for diffusion probabilistic model sampling in around 10 steps. *NeurIPS*, 35: 5775–5787.
- Lu, C.; Zhou, Y.; Bao, F.; Chen, J.; Li, C.; and Zhu, J. 2022b. Dpm-solver++: Fast solver for guided sampling of diffusion probabilistic models. *arXiv preprint arXiv:2211.01095*.
- Lu, C.; Zhou, Y.; Bao, F.; Chen, J.; Li, C.; and Zhu, J. 2022c. Dpm-solver++: Fast solver for guided sampling of diffusion probabilistic models. *arXiv preprint arXiv:2211.01095*.
- Lu, X.; Yuan, H.; Yan, P.; Yuan, Y.; and Li, X. 2012. Geometry constrained sparse coding for single image super-resolution. In *CVPR*.
- Lu, X.; Yuan, Y.; and Yan, P. 2013. Image super-resolution via double sparsity regularized manifold learning. *TCSVT*.
- Luo, S.; Tan, Y.; Huang, L.; Li, J.; and Zhao, H. 2023a. Latent consistency models: Synthesizing high-resolution images with few-step inference. *arXiv preprint arXiv:2310.04378*.
- Luo, X.; Xie, Y.; Zhang, Y.; Qu, Y.; Li, C.; and Fu, Y. 2020. LatticeNet: Towards Lightweight Image Super-resolution with Lattice Block. In *ECCV*.
- Luo, Z.; Gustafsson, F. K.; Zhao, Z.; Sjölund, J.; and Schön, T. B. 2023b. Image Restoration with Mean-Reverting Stochastic Differential Equations. In *ICML*.
- Ma, K.; Duanmu, Z.; Wu, Q.; Wang, Z.; Yong, H.; Li, H.; and Zhang, L. 2016. Waterloo exploration database: New challenges for image quality assessment models. *TIP*.
- Magid, S. A.; Zhang, Y.; Wei, D.; Jang, W.-D.; Lin, Z.; Fu, Y.; and Pfister, H. 2021. Dynamic high-pass filtering and multi-spectral attention for image super-resolution. In *ICCV*.
- Martin, D.; Fowlkes, C.; Tal, D.; and Malik, J. 2001. A database of human segmented natural images and its application to evaluating segmentation algorithms and measuring ecological statistics. In *ICCV*.
- Matsui, Y.; Ito, K.; Aramaki, Y.; Fujimoto, A.; Ogawa, T.; Yamasaki, T.; and Aizawa, K. 2017. Sketch-based manga retrieval using manga109 dataset. *Multimedia Tools and Applications*.
- Mei, K.; Talebi, H.; Ardakani, M.; Patel, V. M.; Milanfar, P.; and Delbracio, M. 2025. The power of context: How multimodality improves image super-resolution. In *CVPR*, 23141–23152.
- Mei, Y.; Fan, Y.; and Zhou, Y. 2021. Image super-resolution with non-local sparse attention. In *CVPR*.
- Mei, Y.; Fan, Y.; Zhou, Y.; Huang, L.; Huang, T. S.; and Shi, H. 2020a. Image Super-Resolution with Cross-Scale Non-Local Attention and Exhaustive Self-Exemplars Mining. In *CVPR*.
- Mei, Y.; Fan, Y.; Zhou, Y.; Huang, L.; Huang, T. S.; and Shi, H. 2020b. Image Super-Resolution with Cross-Scale Non-Local Attention and Exhaustive Self-Exemplars Mining. In *CVPR*.
- Meng, C.; Rombach, R.; Gao, R.; Kingma, D.; Ermon, S.; Ho, J.; and Salimans, T. 2023. On distillation of guided diffusion models. In *CVPR*, 14297–14306.
- Miech, A.; Laptev, I.; and Sivic, J. 2017. Learnable pooling with Context Gating for video classification. *arXiv preprint arXiv:1706.06905*.
- Mildenhall, B.; Barron, J. T.; Chen, J.; Sharlet, D.; Ng, R.; and Carroll, R. 2018. Burst denoising with kernel prediction networks. In *CVPR*.
- Mittal, D.; Bhardwaj, S.; Khapra, M. M.; and Ravindran, B. 2018. Recovering from random pruning: On the plasticity of deep convolutional neural networks. In *WACV*.
- Mnih, V.; Heess, N.; Graves, A.; and Kavukcuoglu, K. 2014. Recurrent models of visual attention. In *NeurIPS*.
- Molchanov, P.; Mallya, A.; Tyree, S.; Frosio, I.; and Kautz, J. 2019. Importance Estimation for Neural Network Pruning. In *CVPR*.

- Molchanov, P.; Tyree, S.; and Karras, T. 2017. Pruning Convolutional Neural Networks for Resource Efficient Inference. In *ICLR*.
- Mou, C.; Wang, X.; Xie, L.; Zhang, J.; Qi, Z.; Shan, Y.; and Qie, X. 2023. T2i-adapter: Learning adapters to dig out more controllable ability for text-to-image diffusion models. *arXiv preprint arXiv:2302.08453*.
- Mou, C.; Wu, Y.; Wang, X.; Dong, C.; Zhang, J.; and Shan, Y. 2022. Metric learning based interactive modulation for real-world super-resolution. In *ECCV*.
- Mou, C.; Zhang, J.; and Wu, Z. 2021. Dynamic attentive graph learning for image restoration. In *ICCV*.
- Nair, V.; and Hinton, G. E. 2010. Rectified linear units improve restricted boltzmann machines. In *ICML*.
- Neal, R. M. 2001. Annealed importance sampling. *Statistics and computing*, 11: 125–139.
- Newell, A. 1980. Physical symbol systems. *Cognitive science*.
- Nguyen, T. H.; and Tran, A. 2024. Swiftbrush: One-step text-to-image diffusion model with variational score distillation. In *CVPR*.
- Nichol, A. Q.; and Dhariwal, P. 2021. Improved denoising diffusion probabilistic models. In *ICML*, 8162–8171. PMLR.
- Niu, B.; Wen, W.; Ren, W.; Zhang, X.; Yang, L.; Wang, S.; Zhang, K.; Cao, X.; and Shen, H. 2020. Single Image Super-Resolution via a Holistic Attention Network. In *ECCV*.
- Olshausen, B. A.; and Field, D. J. 1997. Sparse coding with an overcomplete basis set: A strategy employed by V1? *Vision research*, 37(23): 3311–3325.
- Pan, X.; Zhan, X.; Dai, B.; Lin, D.; Loy, C. C.; and Luo, P. 2021. Exploiting deep generative prior for versatile image restoration and manipulation. *IEEE PAMI*, 44(11): 7474–7489.
- Parmar, G.; Park, T.; Narasimhan, S.; and Zhu, J.-Y. 2024. One-Step Image Translation with Text-to-Image Models. *arXiv preprint arXiv:2403.12036*.
- Paszke, A.; Gross, S.; Chintala, S.; Chanan, G.; Yang, E.; DeVito, Z.; Lin, Z.; Desmaison, A.; Antiga, L.; and Lerer, A. 2017. Automatic differentiation in PyTorch.
- Paszke, A.; Gross, S.; Massa, F.; Lerer, A.; Bradbury, J.; Chanan, G.; Killeen, T.; Lin, Z.; Gimelshein, N.; Antiga, L.; et al. 2019. Pytorch: An imperative style, high-performance deep learning library. In *NeurIPS*.
- Peleg, T.; and Elad, M. 2014. A statistical prediction model based on sparse representations for single image super-resolution. *TIP*.
- Pérez-Pellitero, E.; Salvador, J.; Ruiz-Hidalgo, J.; and Rosenhahn, B. 2016a. Antipodally invariant metrics for fast regression-based super-resolution. *TIP*.
- Pérez-Pellitero, E.; Salvador, J.; Ruiz-Hidalgo, J.; and Rosenhahn, B. 2016b. Psyco: Manifold span reduction for super resolution. In *CVPR*.
- Plotz, T.; and Roth, S. 2017. Benchmarking denoising algorithms with real photographs. In *CVPR*.
- Podell, D.; English, Z.; Lacey, K.; Blattmann, A.; Dockhorn, T.; Müller, J.; Penna, J.; and Rombach, R. 2023. Sdxl: Improving latent diffusion models for high-resolution image synthesis. *arXiv preprint arXiv:2307.01952*.
- Poole, B.; Jain, A.; Barron, J. T.; and Mildenhall, B. 2022. Dreamfusion: Text-to-3d using 2d diffusion. *arXiv preprint arXiv:2209.14988*.
- Radford, A.; Kim, J. W.; Hallacy, C.; Ramesh, A.; Goh, G.; Agarwal, S.; Sastry, G.; Askell, A.; Mishkin, P.; Clark, J.; et al. 2021. Learning transferable visual models from natural language supervision. In *ICML*.
- Raghu, M.; Unterthiner, T.; Kornblith, S.; Zhang, C.; and Dosovitskiy, A. 2021. Do vision transformers see like convolutional neural networks? In *NeurIPS*.
- Redmon, J.; Divvala, S.; Girshick, R.; and Farhadi, A. 2016. You only look once: Unified, real-time object detection. In *CVPR*, 779–788.
- Reed, R. 1993. Pruning algorithms – a survey. *IEEE Transactions on Neural Networks*.
- Ren, C.; He, X.; Wang, C.; and Zhao, Z. 2021a. Adaptive consistency prior based deep network for image denoising. In *CVPR*.
- Ren, H.; El-Khamy, M.; and Lee, J. 2017. Image super resolution based on fusing multiple convolution neural networks. In *CVPRW*.
- Ren, S.; Zhou, D.; He, S.; Feng, J.; and Wang, X. 2021b. Shunted Self-Attention via Multi-Scale Token Aggregation. *arXiv preprint arXiv:2111.15193*.
- Rombach, R.; Blattmann, A.; Lorenz, D.; Esser, P.; and Ommer, B. 2022a. High-resolution image synthesis with latent diffusion models. In *CVPR*, 10684–10695.
- Rombach, R.; Blattmann, A.; Lorenz, D.; Esser, P.; and Ommer, B. 2022b. High-Resolution Image Synthesis With Latent Diffusion Models. In *CVPR*.
- Ronneberger, O.; Fischer, P.; and Brox, T. 2015. U-net: Convolutional networks for biomedical image segmentation. In *MICCAI*.
- Roth, S.; and Black, M. J. 2009. Fields of experts. *IJCV*, 82(2): 205–229.
- Rothe, R.; Timofte, R.; and Van, L. 2015. Efficient regression priors for reducing image compression artifacts. In *Proc. Int. Conf. Image Process.*, 1543–1547.
- Roweis, S. T.; and Saul, L. K. 2000. Nonlinear dimensionality reduction by locally linear embedding. *Science*.
- Russakovsky, O.; Deng, J.; Su, H.; Krause, J.; Satheesh, S.; Ma, S.; Huang, Z.; Karpathy, A.; Khosla, A.; Bernstein, M.; et al. 2015. Imagenet large scale visual recognition challenge. *IJCV*.
- Saharia, C.; Chan, W.; Saxena, S.; Li, L.; Whang, J.; Denton, E. L.; Ghasemipour, K.; Gontijo Lopes, R.; Karagol Ayan, B.; Salimans, T.; et al. 2022a. Photorealistic text-to-image diffusion models with deep language understanding. *NeurIPS*.
- Saharia, C.; Ho, J.; Chan, W.; Salimans, T.; Fleet, D. J.; and Norouzi, M. 2022b. Image super-resolution via iterative refinement. *IEEE PAMI*.
- Sajjadi, M. S.; Schölkopf, B.; and Hirsch, M. 2017. Enhancenet: Single image super-resolution through automated texture synthesis. In *ICCV*.
- Salem, F.; and Yagle, A. E. 2013. Non-Parametric super-resolution using a Bi-sensor camera. *TMM*, 15(1): 27–40.
- Salimans, T.; and Ho, J. 2022. Progressive distillation for fast sampling of diffusion models. *arXiv preprint arXiv:2202.00512*.
- Salimans, T.; and Kingma, D. P. 2016. Weight Normalization: A Simple Reparameterization to Accelerate Training of Deep Neural Networks. In *NeurIPS*.
- Santoro, A.; Raposo, D.; Barrett, D. G.; Malinowski, M.; Pascanu, R.; Battaglia, P.; and Lillicrap, T. 2017. A simple neural network module for relational reasoning. In *NeurIPS*.
- Sauer, A.; Boesel, F.; Dockhorn, T.; Blattmann, A.; Esser, P.; and Rombach, R. 2024. Fast High-Resolution Image Synthesis with Latent Adversarial Diffusion Distillation. *arXiv preprint arXiv:2403.12015*.
- Sauer, A.; Lorenz, D.; Blattmann, A.; and Rombach, R. 2023. Adversarial diffusion distillation. *arXiv preprint arXiv:2311.17042*.

- Schulter, S.; Leistner, C.; and Bischof, H. 2015. Fast and Accurate Image Upscaling With Super-Resolution Forests. In *CVPR*.
- Schulter, S.; Leistner, C.; Wohlhart, P.; Roth, P. M.; and Bischof, H. 2013. Alternating regression forests for object detection and pose estimation. In *ICCV*.
- Sheikh, H. R.; and Bovik, A. C. 2006. Image information and visual quality. *TIP*.
- Sheikh, H. R.; Bovik, A. C.; and De Veciana, G. 2005. An information fidelity criterion for image quality assessment using natural scene statistics. *TIP*.
- Sheikh, H. R.; Sabir, M. F.; and Bovik, A. C. 2006. A statistical evaluation of recent full reference image quality assessment algorithms. *TIP*.
- Shen, J.; Shen, J.; Mei, T.; and Gao, X. 2016. Landmark Reranking for Smart Travel Guide Systems by Combining and Analyzing Diverse Media. *IEEE Trans. Syst., Man, Cybern., Syst.*, 46(11): 1492–1504.
- Shi, W.; Caballero, J.; Huszár, F.; Totz, J.; Aitken, A. P.; Bishop, R.; Rueckert, D.; and Wang, Z. 2016. Real-time single image and video super-resolution using an efficient sub-pixel convolutional neural network. In *CVPR*.
- Shi, W.; Caballero, J.; Ledig, C.; Zhuang, X.; Bai, W.; Bhatia, K.; de Marvao, A. M. S. M.; Dawes, T.; O'Regan, D.; and Rueckert, D. 2013. Cardiac image super-resolution with global correspondence using multi-atlas patchmatch. In *MICCAI*.
- Simonyan, K.; and Zisserman, A. 2014. Very deep convolutional networks for large-scale image recognition. *arXiv preprint arXiv:1409.1556*.
- Singer, U.; Polyak, A.; Hayes, T.; Yin, X.; An, J.; Zhang, S.; Hu, Q.; Yang, H.; Ashual, O.; Gafni, O.; et al. 2022. Make-a-video: Text-to-video generation without text-video data. *arXiv preprint arXiv:2209.14792*.
- Sohl-Dickstein, J.; Weiss, E.; Maheswaranathan, N.; and Ganguli, S. 2015. Deep unsupervised learning using nonequilibrium thermodynamics. In *ICML*.
- Song, J.; Meng, C.; and Ermon, S. 2021. Denoising diffusion implicit models. In *ICLR*.
- Song, J.; Meng, C.; and Ermon, S. 2022. Denoising diffusion implicit models. In *ICLR*.
- Song, J.; Vahdat, A.; Mardani, M.; and Kautz, J. 2022. Pseudoinverse-guided diffusion models for inverse problems. In *ICLR*.
- Song, Y.; Dhariwal, P.; Chen, M.; and Sutskever, I. 2023. Consistency models. In *ICML*.
- Song, Y.; Sohl-Dickstein, J.; Kingma, D. P.; Kumar, A.; Ermon, S.; and Poole, B. 2020. Score-based generative modeling through stochastic differential equations. *arXiv preprint arXiv:2011.13456*.
- Sun, D.; and Cham, W.-K. 2007. Postprocessing of low bit-rate block DCT coded images based on a fields of experts prior. *TIP*.
- Sun, H.; Li, W.; Liu, J.; Chen, H.; Pei, R.; Zou, X.; Yan, Y.; and Yang, Y. 2023. CoSeR: Bridging Image and Language for Cognitive Super-Resolution. *arXiv preprint arXiv:2311.16512*.
- Sun, J.; Xu, Z.; and Shum, H.-Y. 2008. Image super-resolution using gradient profile prior. In *CVPR*.
- Sun, J.; Zhu, J.; and Tappen, M. F. 2010. Context-constrained hallucination for image super-resolution. In *CVPR*.
- Sun, L.; Wu, R.; Ma, Z.; Liu, S.; Yi, Q.; and Zhang, L. 2025. Pixel-level and semantic-level adjustable super-resolution: A dual-lora approach. In *Proceedings of the Computer Vision and Pattern Recognition Conference*, 2333–2343.
- Suo, J.; Lin, L.; Shan, S.; Chen, X.; and Gao, W. 2011. High-Resolution Face Fusion for Gender Conversion. *IEEE Trans. Syst., Man, Cybern. A, Syst., Humans*, 41(2): 226–237.
- Sze, V.; Chen, Y.-H.; Yang, T.-J.; and Emer, J. S. 2017. Efficient processing of deep neural networks: A tutorial and survey. *Proceedings of the IEEE*, 105(12): 2295–2329.
- Szegedy, C.; Ioffe, S.; Vanhoucke, V.; and Alemi, A. A. 2017. Inception-v4, Inception-ResNet and the Impact of Residual Connections on Learning. In *AAAI*.
- Tai, Y.; Yang, J.; and Liu, X. 2017. Image Super-Resolution via Deep Recursive Residual Network. In *CVPR*.
- Tai, Y.; Yang, J.; Liu, X.; and Xu, C. 2017. MemNet: A Persistent Memory Network for Image Restoration. In *ICCV*.
- Tancik, M.; Srinivasan, P.; Mildenhall, B.; Fridovich-Keil, S.; Raghavan, N.; Singh, U.; Ramamoorthi, R.; Barron, J.; and Ng, R. 2020. Fourier features let networks learn high frequency functions in low dimensional domains. *NeurIPS*, 33: 7537–7547.
- Tang, Y.; Chen, H.; Liu, Z.; Song, B.; and Wang, Q. 2016. Example-based super-resolution via social images. *Neurocomputing*.
- Tang, Y.; Yan, P.; Yuan, Y.; and Li, X. 2011. Single-image super-resolution via local learning. *Int. J. Mach. Learn. Cybern.*, 2(1): 15–23.
- Timofte, R.; Agustsson, E.; Van Gool, L.; Yang, M.-H.; and Zhang, L. 2017a. Ntire 2017 challenge on single image super-resolution: Methods and results. In *CVPRW*.
- Timofte, R.; Agustsson, E.; Van Gool, L.; Yang, M.-H.; Zhang, L.; Lim, B.; Son, S.; Kim, H.; Nah, S.; Lee, K. M.; et al. 2017b. Ntire 2017 challenge on single image super-resolution: Methods and results. In *CVPRW*.
- Timofte, R.; De, V.; and Gool, L. V. 2013. Anchored neighborhood regression for fast example-based super-resolution. In *ICCV*.
- Timofte, R.; De Smet, V.; and Van Gool, L. 2014. A+: Adjusted Anchored Neighborhood Regression for Fast Super-Resolution. In *ACCV*.
- Timofte, R.; Rothe, R.; and Van Gool, L. 2016. Seven ways to improve example-based single image super resolution. In *CVPR*.
- Tong, T.; Li, G.; Liu, X.; and Gao, Q. 2017. Image Super-Resolution Using Dense Skip Connections. In *ICCV*.
- Tropp, J. A.; and Gilbert, A. C. 2007. Signal recovery from random measurements via orthogonal matching pursuit. *TIT*.
- Tsai, F.-J.; Peng, Y.-T.; Lin, Y.-Y.; Tsai, C.-C.; and Lin, C.-W. 2022. Stripformer: Strip transformer for fast image deblurring. In *ECCV*.
- Tschumperle, D.; and Deriche, R. 2005. Vector-valued image regularization with PDEs: A common framework for different applications. *PAMI*.
- Tu, Z.; Talebi, H.; Zhang, H.; Yang, F.; Milanfar, P.; Bovik, A.; and Li, Y. 2022. Maxvit: Multi-axis vision transformer. In *ECCV*.
- Vaswani, A.; Ramachandran, P.; Srinivas, A.; Parmar, N.; Hechtman, B.; and Shlens, J. 2021. Scaling local self-attention for parameter efficient visual backbones. In *CVPR*.
- Vaswani, A.; Shazeer, N.; Parmar, N.; Uszkoreit, J.; Jones, L.; Gomez, A. N.; Kaiser, Ł.; and Polosukhin, I. 2017. Attention is all you need. In *NeurIPS*.
- Venugopalan, S.; Rohrbach, M.; Darrell, T.; and Saenko, K. 2015. Sequence to sequence-video to text. In *ICCV*.
- Wang, C.; Grosse, R.; Fidler, S.; and Zhang, G. 2019a. EigenDamage: Structured Pruning in the Kronecker-Factored Eigenbasis. In *ICML*.

- Wang, C.; Zhou, J.; and Liu, S. 2013. Adaptive non-local means filter for image deblocking. *Signal Process.: Image Commun.*, 28(5): 522–530.
- Wang, F.; Jiang, M.; Qian, C.; Yang, S.; Li, C.; Zhang, H.; Wang, X.; and Tang, X. 2017. Residual attention network for image classification. In *CVPR*.
- Wang, H.; Hu, X.; Zhang, Q.; Wang, Y.; Yu, L.; and Hu, H. 2019b. Structured pruning for efficient convolutional neural networks via incremental regularization. *IEEE Journal of Selected Topics in Signal Processing*, 14(4): 775–788.
- Wang, H.; Qin, C.; Zhang, Y.; and Fu, Y. 2021a. Neural Pruning via Growing Regularization. In *ICLR*.
- Wang, J.; Chan, K. C.; and Loy, C. C. 2023a. Exploring clip for assessing the look and feel of images. In *AAAI*, volume 37, 2555–2563.
- Wang, J.; Chan, K. C.; and Loy, C. C. 2023b. Exploring clip for assessing the look and feel of images. In *AAAI*.
- Wang, J.; Yue, Z.; Zhou, S.; Chan, K. C.; and Loy, C. C. 2024a. Exploiting diffusion prior for real-world image super-resolution. *International Journal of Computer Vision*, 1–21.
- Wang, L.; Xiang, S.; Meng, G.; Wu, H.-Y.; and Pan, C. 2013. Edge-Directed Single-Image Super-Resolution Via Adaptive Gradient Magnitude Self-Interpolation. *TCSVT*.
- Wang, Q.; and Yuan, Y. 2014. High quality image resizing. *Neurocomputing*.
- Wang, T.; and Zhai, G. 2008. JPEG2000 image postprocessing with novel trilateral deringing filter. *Opt. Eng.*, 47(2): 027005–027005.
- Wang, W.; Xie, E.; Li, X.; Fan, D.-P.; Song, K.; Liang, D.; Lu, T.; Luo, P.; and Shao, L. 2021b. Pyramid vision transformer: A versatile backbone for dense prediction without convolutions. In *ICCV*.
- Wang, W.; Yao, L.; Chen, L.; Lin, B.; Cai, D.; He, X.; and Liu, W. 2022a. CrossFormer: A Versatile Vision Transformer Hinging on Cross-scale Attention. In *ICLR*.
- Wang, X.; Girshick, R.; Gupta, A.; and He, K. 2018a. Non-local neural networks. In *CVPR*.
- Wang, X.; and Gupta, A. 2018. Videos as space-time region graphs. In *ECCV*.
- Wang, X.; Xie, L.; Dong, C.; and Shan, Y. 2021c. Real-esrgan: Training real-world blind super-resolution with pure synthetic data. In *ICCV*.
- Wang, X.; Xie, L.; Dong, C.; and Shan, Y. 2021d. Real-esrgan: Training real-world blind super-resolution with pure synthetic data. In *ICCV*.
- Wang, X.; Yu, K.; Dong, C.; and Loy, C. C. 2018b. Recovering realistic texture in image super-resolution by deep spatial feature transform. In *CVPR*.
- Wang, X.; Yu, K.; Wu, S.; Gu, J.; Liu, Y.; Dong, C.; Qiao, Y.; and Change Loy, C. 2018c. Esgan: Enhanced super-resolution generative adversarial networks. In *ECCV Workshop*.
- Wang, Y.; Yang, W.; Chen, X.; Wang, Y.; Guo, L.; Chau, L.-P.; Liu, Z.; Qiao, Y.; Kot, A. C.; and Wen, B. 2024b. SinSR: Diffusion-Based Image Super-Resolution in a Single Step. In *CVPR*.
- Wang, Y.; Yu, J.; and Zhang, J. 2023. Zero-shot image restoration using denoising diffusion null-space model. In *ICLR*.
- Wang, Z.; Bovik, A. C.; Sheikh, H. R.; and Simoncelli, E. P. 2004a. Image quality assessment: from error visibility to structural similarity. *IEEE TIP*, 13(4): 600–612.
- Wang, Z.; Bovik, A. C.; Sheikh, H. R.; and Simoncelli, E. P. 2004b. Image quality assessment: from error visibility to structural similarity. *TIP*.
- Wang, Z.; Chen, J.; and Hoi, S. C. 2020. Deep learning for image super-resolution: A survey. *PAMI*.
- Wang, Z.; Cun, X.; Bao, J.; Zhou, W.; Liu, J.; and Li, H. 2022b. Uformer: A general u-shaped transformer for image restoration. In *CVPR*.
- Wang, Z.; Liu, D.; Yang, J.; Han, W.; and Huang, T. 2015. Deep Networks for Image Super-Resolution with Sparse Prior. In *ICCV*.
- Wang, Z.; Lu, C.; Wang, Y.; Bao, F.; Li, C.; Su, H.; and Zhu, J. 2023a. ProlificDreamer: High-Fidelity and Diverse Text-to-3D Generation with Variational Score Distillation. *arXiv preprint arXiv:2305.16213*.
- Wang, Z.; Lu, C.; Wang, Y.; Bao, F.; Li, C.; Su, H.; and Zhu, J. 2024c. Prolificdreamer: High-fidelity and diverse text-to-3d generation with variational score distillation. In *NeurIPS*.
- Wang, Z.; Simoncelli, E. P.; and Bovik, A. C. 2004. Multiscale structural similarity for image quality assessment. In *Signals, Systems and Computers, 2004. Conference Record of the Thirty-Seventh Asilomar Conference on*.
- Wang, Z.; Zheng, H.; He, P.; Chen, W.; and Zhou, M. 2023b. Diffusion-gan: Training gans with diffusion. In *ICLR*.
- Wei, P.; Xie, Z.; Lu, H.; Zhan, Z.; Ye, Q.; Zuo, W.; and Lin, L. 2020a. Component divide-and-conquer for real-world image super-resolution. In *ECCV*, 101–117. Springer.
- Wei, P.; Xie, Z.; Lu, H.; Zhan, Z.; Ye, Q.; Zuo, W.; and Lin, L. 2020b. Component divide-and-conquer for real-world image super-resolution. In *ECCV*.
- Wen, W.; Wu, C.; Wang, Y.; Chen, Y.; and Li, H. 2016. Learning structured sparsity in deep neural networks. In *NeurIPS*.
- Woo, S.; Park, J.; Lee, J.-Y.; and So Kweon, I. 2018. Cbam: Convolutional block attention module. In *ECCV*.
- Wu, F.; Fan, A.; Baevski, A.; Dauphin, Y. N.; and Auli, M. 2019. Pay less attention with lightweight and dynamic convolutions. *arXiv preprint arXiv:1901.10430*.
- Wu, J. Z.; Ge, Y.; Wang, X.; Lei, S. W.; Gu, Y.; Shi, Y.; Hsu, W.; Shan, Y.; Qie, X.; and Shou, M. Z. 2023. Tune-a-video: One-shot tuning of image diffusion models for text-to-video generation. In *ICCV*, 7623–7633.
- Wu, R.; Sun, L.; Ma, Z.; and Zhang, L. 2024a. One-step effective diffusion network for real-world image super-resolution. *NeurIPS*, 37: 92529–92553.
- Wu, R.; Yang, T.; Sun, L.; Zhang, Z.; Li, S.; and Zhang, L. 2024b. Seesr: Towards semantics-aware real-world image super-resolution. In *CVPR*.
- Xia, B.; Zhang, Y.; Wang, S.; Wang, Y.; Wu, X.; Tian, Y.; Yang, W.; and Van Gool, L. 2023. Diffir: Efficient diffusion model for image restoration. In *ICCV*.
- Xiao, H.; Lee, L. H.; and Chen, C.-H. 2015. Optimal Budget Allocation Rule for Simulation Optimization Using Quadratic Regression in Partitioned Domains. *IEEE Trans. Syst., Man, Cybern., Syst.*, 45(7): 1047–1062.
- Xie, E.; Wang, W.; Yu, Z.; Anandkumar, A.; Alvarez, J. M.; and Luo, P. 2021. SegFormer: Simple and efficient design for semantic segmentation with transformers. In *NeurIPS*.
- Xie, L.; Wang, X.; Chen, X.; Li, G.; Shan, Y.; Zhou, J.; and Dong, C. 2023. Desra: detect and delete the artifacts of gan-based real-world super-resolution models. *arXiv preprint arXiv:2307.02457*.

- Xiong, Z.; Xu, D.; Sun, X.; and Wu, F. 2013. Example-based super-resolution with soft information and decision. *TMM*, 15(6): 1458–1465.
- Xu, H.; Zhai, G.; and Yang, X. 2013. Single image super-resolution with detail enhancement based on local fractal analysis of gradient. *TCSVT*.
- Yan, H.; Zhang, C.; and Wu, M. 2022. Lawin Transformer: Improving Semantic Segmentation Transformer with Multi-Scale Representations via Large Window Attention. *arXiv preprint arXiv:2201.01615*.
- Yang, C.-Y.; Ma, C.; and Yang, M.-H. 2014. Single-image super-resolution: A benchmark. In *ECCV*, 372–386. Springer.
- Yang, C.-Y.; and Yang, M.-H. 2013. Fast direct super-resolution by simple functions. In *ICCV*.
- Yang, J.; Li, C.; Zhang, P.; Dai, X.; Xiao, B.; Yuan, L.; and Gao, J. 2021. Focal self-attention for local-global interactions in vision transformers. In *NeurIPS*.
- Yang, J.; Wright, J.; Huang, T.; and Ma, Y. 2008. Image super-resolution as sparse representation of raw image patches. In *CVPR*.
- Yang, J.; Wright, J.; Huang, T. S.; and Ma, Y. 2010. Image super-resolution via sparse representation. *IEEE TIP*.
- Yang, M.-C.; and Wang, Y.-C. F. 2013. A self-learning approach to single image super-resolution. *TMM*, 15(3): 498–508.
- Yang, R.; Ma, H.; Wu, J.; Tang, Y.; Xiao, X.; Zheng, M.; and Li, X. 2022a. Scalablelevit: Rethinking the context-oriented generalization of vision transformer. In *ECCV*.
- Yang, S.; Wu, T.; Shi, S.; Lao, S.; Gong, Y.; Cao, M.; Wang, J.; and Yang, Y. 2022b. Maniqa: Multi-dimension attention network for no-reference image quality assessment. In *CVPR*, 1191–1200.
- Yang, S.; Wu, T.; Shi, S.; Lao, S.; Gong, Y.; Cao, M.; Wang, J.; and Yang, Y. 2022c. Maniqa: Multi-dimension attention network for no-reference image quality assessment. In *CVPR*.
- Yang, T.; Wu, R.; Ren, P.; Xie, X.; and Zhang, L. 2024. Pixel-aware stable diffusion for realistic image super-resolution and personalized stylization. In *ECCV*.
- Yang, W.; Tian, Y.; Zhou, F.; Liao, Q.; Chen, H.; and Zheng, C. 2016. Consistent Coding Scheme for Single-Image Super-Resolution Via Independent Dictionaries. *TMM*, 18(3): 313–325.
- Yang, W.; Wang, X.; Farhadi, A.; Gupta, A.; and Mottaghi, R. 2019. Visual semantic navigation using scene priors. *ICLR*.
- Yang, W.; Yuan, T.; Wang, W.; Zhou, F.; and Liao, Q. 2017. Single-Image Super-Resolution by Subdictionary Coding and Kernel Regression. *IEEE Trans. Syst., Man, Cybern., Syst.*, PP(99): 1–11.
- Yang, Y.; Galatsanos, N. P.; and Katsaggelos, A. K. 1995. Projection-based spatially adaptive reconstruction of block-transform compressed images. *TIP*.
- Yang, Y.; Zhong, Z.; Shen, T.; and Lin, Z. 2018. Convolutional neural networks with alternately updated clique. In *CVPR*.
- Yao, T.; Pan, Y.; Li, Y.; and Mei, T. 2018. Exploring visual relationship for image captioning. In *ECCV*.
- Ye, J.; Lu, X.; Lin, Z.; and Wang, J. Z. 2018. Rethinking the smaller-norm-less-informative assumption in channel pruning of convolution layers. In *ICLR*.
- Yim, C.; and Bovik, A. C. 2010. Quality assessment of deblocked images. *TIP*.
- Yin, T.; Gharbi, M.; Park, T.; Zhang, R.; Shechtman, E.; Durand, F.; and Freeman, W. T. 2024a. Improved Distribution Matching Distillation for Fast Image Synthesis. *arXiv preprint arXiv:2405.14867*.
- Yin, T.; Gharbi, M.; Zhang, R.; Shechtman, E.; Durand, F.; Freeman, W. T.; and Park, T. 2024b. One-step diffusion with distribution matching distillation. In *CVPR*, 6613–6623.
- Yin, T.; Gharbi, M.; Zhang, R.; Shechtman, E.; Durand, F.; Freeman, W. T.; and Park, T. 2024c. One-step diffusion with distribution matching distillation. In *CVPR*.
- Yu, F.; Gu, J.; Li, Z.; Hu, J.; Kong, X.; Wang, X.; He, J.; Qiao, Y.; and Dong, C. 2024. Scaling Up to Excellence: Practicing Model Scaling for Photo-Realistic Image Restoration In the Wild. In *CVPR*.
- Yuan, K.; Guo, S.; Liu, Z.; Zhou, A.; Yu, F.; and Wu, W. 2021. Incorporating convolution designs into visual transformers. In *CVPR*.
- Yue, Z.; Liao, K.; and Loy, C. C. 2025. Arbitrary-steps image super-resolution via diffusion inversion. In *CVPR*, 23153–23163.
- Yue, Z.; and Loy, C. C. 2024. Difface: Blind face restoration with diffused error contraction. *IEEE PAMI*.
- Yue, Z.; Wang, J.; and Loy, C. C. 2023. Resshift: Efficient diffusion model for image super-resolution by residual shifting. In *NeurIPS*.
- Yue, Z.; Wang, J.; and Loy, C. C. 2024a. Efficient diffusion model for image restoration by residual shifting. *IEEE PAMI*.
- Yue, Z.; Wang, J.; and Loy, C. C. 2024b. Resshift: Efficient diffusion model for image super-resolution by residual shifting. In *NeurIPS*.
- Yue, Z.; Yong, H.; Zhao, Q.; Zhang, L.; Meng, D.; and Wong, K.-Y. K. 2024. Deep variational network toward blind image restoration. *IEEE PAMI*.
- Yue, Z.; Zhao, Q.; Zhang, L.; and Meng, D. 2020. Dual adversarial network: Toward real-world noise removal and noise generation. In *ECCV*.
- Zamir, A. R.; Wu, T.-L.; Sun, L.; Shen, W. B.; Shi, B. E.; Malik, J.; and Savarese, S. 2017. Feedback networks. In *CVPR*.
- Zamir, S. W.; Arora, A.; Khan, S.; Hayat, M.; Khan, F. S.; and Yang, M.-H. 2022a. Restormer: Efficient transformer for high-resolution image restoration. In *CVPR*, 5728–5739.
- Zamir, S. W.; Arora, A.; Khan, S.; Hayat, M.; Khan, F. S.; and Yang, M.-H. 2022b. Restormer: Efficient Transformer for High-Resolution Image Restoration. In *CVPR*.
- Zamir, S. W.; Arora, A.; Khan, S.; Hayat, M.; Khan, F. S.; Yang, M.-H.; and Shao, L. 2020a. Cycleisp: Real image restoration via improved data synthesis. In *CVPR*.
- Zamir, S. W.; Arora, A.; Khan, S.; Hayat, M.; Khan, F. S.; Yang, M.-H.; and Shao, L. 2020b. Learning enriched features for real image restoration and enhancement. In *ECCV*.
- Zamir, S. W.; Arora, A.; Khan, S.; Hayat, M.; Khan, F. S.; Yang, M.-H.; and Shao, L. 2021. Multi-stage progressive image restoration. In *CVPR*.
- Zeyde, R.; Elad, M.; and Protter, M. 2010. On single image scale-up using sparse-representations. In *Proc. 7th Int. Conf. Curves Surf.*
- Zhang, A.; Yue, Z.; Pei, R.; Ren, W.; and Cao, X. 2024a. Degradation-guided one-step image super-resolution with diffusion priors. *arXiv preprint arXiv:2409.17058*.
- Zhang, A.; Yue, Z.; Pei, R.; Ren, W.; and Cao, X. 2024b. Degradation-guided one-step image super-resolution with diffusion priors. *arXiv preprint arXiv:2409.17058*.
- Zhang, H.; Li, F.; Zou, X.; Liu, S.; Li, C.; Gao, J.; Yang, J.; and Zhang, L. 2023a. A Simple Framework for Open-Vocabulary Segmentation and Detection. In *CVPR*.
- Zhang, H.; and Patel, V. M. 2018a. Densely Connected Pyramid Dehazing Network. In *CVPR*.

- Zhang, H.; and Patel, V. M. 2018b. Density-aware Single Image De-raining using a Multi-stream Dense Network. In *CVPR*.
- Zhang, H.; Sindagi, V.; and Patel, V. M. 2017. Image de-raining using a conditional generative adversarial network. *arXiv preprint arXiv:1701.05957*.
- Zhang, J.; Herrmann, C.; Hur, J.; Cabrera, L. P.; Jampani, V.; Sun, D.; and Yang, M.-H. 2023b. A Tale of Two Features: Stable Diffusion Complements DINO for Zero-Shot Semantic Correspondence. *arXiv preprint arXiv:2305.15347*.
- Zhang, K.; Gao, X.; Tao, D.; and Li, X. 2012. Single image super-resolution with non-local means and steering kernel regression. *TIP*.
- Zhang, K.; Li, Y.; Zuo, W.; Zhang, L.; Van Gool, L.; and Timofte, R. 2021a. Plug-and-play image restoration with deep denoiser prior. *PAMI*.
- Zhang, K.; Liang, J.; Van Gool, L.; and Timofte, R. 2021b. Designing a practical degradation model for deep blind image super-resolution. In *ICCV*, 4791–4800.
- Zhang, K.; Sun, M.; Han, X.; Yuan, X.; Guo, L.; and Liu, T. 2017a. Residual networks of residual networks: Multilevel residual networks. *TCSVT*.
- Zhang, K.; Tao, D.; Gao, X.; Li, X.; and Xiong, Z. 2015a. Learning multiple linear mappings for efficient single image super-resolution. *TIP*.
- Zhang, K.; Zuo, W.; Chen, Y.; Meng, D.; and Zhang, L. 2017b. Beyond a gaussian denoiser: Residual learning of deep cnn for image denoising. *TIP*.
- Zhang, K.; Zuo, W.; Gu, S.; and Zhang, L. 2017c. Learning Deep CNN Denoiser Prior for Image Restoration. In *CVPR*.
- Zhang, K.; Zuo, W.; and Zhang, L. 2018. Learning a single convolutional super-resolution network for multiple degradations. In *CVPR*.
- Zhang, L.; Rao, A.; and Agrawala, M. 2023. Adding conditional control to text-to-image diffusion models. In *ICCV*, 3836–3847.
- Zhang, L.; and Wu, X. 2006. An edge-guided image interpolation algorithm via directional filtering and data fusion. *TIP*.
- Zhang, L.; Yang, M.; and Feng, X. 2011. Sparse representation or collaborative representation: Which helps face recognition? In *ICCV*.
- Zhang, L.; Zhang, L.; and Bovik, A. C. 2015a. A feature-enriched completely blind image quality evaluator. *IEEE TIP*, 24(8): 2579–2591.
- Zhang, L.; Zhang, L.; and Bovik, A. C. 2015b. A feature-enriched completely blind image quality evaluator. *TIP*.
- Zhang, L.; Zhang, L.; Mou, X.; and Zhang, D. 2011. FSIM: a feature similarity index for image quality assessment. *TIP*.
- Zhang, R.; Isola, P.; Efros, A. A.; Shechtman, E.; and Wang, O. 2018a. The unreasonable effectiveness of deep features as a perceptual metric. In *CVPR*, 586–595.
- Zhang, R.; Isola, P.; Efros, A. A.; Shechtman, E.; and Wang, O. 2018b. The unreasonable effectiveness of deep features as a perceptual metric. In *CVPR*.
- Zhang, X.; Zeng, H.; Guo, S.; and Zhang, L. 2022. Efficient long-range attention network for image super-resolution. In *ECCV*, 649–667. Springer.
- Zhang, Y.; Fang, C.; Wang, Y.; Wang, Z.; Lin, Z.; Fu, Y.; and Yang, J. 2019a. Multimodal Style Transfer via Graph Cuts. In *ICCV*.
- Zhang, Y.; Gu, K.; Zhang, Y.; Zhang, J.; and Dai, Q. 2015b. Image super-resolution based on dictionary learning and anchored neighborhood regression with mutual incoherence. In *Proc. IEEE Int. Conf. Image Process.*, 591–595.
- Zhang, Y.; Huang, X.; Ma, J.; Li, Z.; Luo, Z.; Xie, Y.; Qin, Y.; Luo, T.; Li, Y.; Liu, S.; et al. 2023c. Recognize Anything: A Strong Image Tagging Model. *arXiv preprint arXiv:2306.03514*.
- Zhang, Y.; Li, K.; Li, K.; Wang, L.; Zhong, B.; and Fu, Y. 2018c. Image super-resolution using very deep residual channel attention networks. In *ECCV*.
- Zhang, Y.; Li, K.; Li, K.; Wang, L.; Zhong, B.; and Fu, Y. 2018d. Image super-resolution using very deep residual channel attention networks. In *ECCV*.
- Zhang, Y.; Li, K.; Li, K.; Zhong, B.; and Fu, Y. 2019b. Residual Non-local Attention Networks for Image Restoration. In *ICLR*.
- Zhang, Y.; Tian, Y.; Kong, Y.; Zhong, B.; and Fu, Y. 2018e. Residual dense network for image super-resolution. In *CVPR*, 2472–2481.
- Zhang, Y.; Tian, Y.; Kong, Y.; Zhong, B.; and Fu, Y. 2018f. Residual Dense Network for Image Super-Resolution. In *CVPR*.
- Zhang, Y.; Tian, Y.; Kong, Y.; Zhong, B.; and Fu, Y. 2020. Residual Dense Network for Image Restoration. *PAMI*.
- Zhang, Y.; Wei, D.; Qin, C.; Wang, H.; Pfister, H.; and Fu, Y. 2021c. Context reasoning attention network for image super-resolution. In *ICCV*.
- Zhang, Y.; Zhang, Y.; Zhang, J.; and Dai, Q. 2016. CCR: clustering and collaborative representation for fast single image super-resolution. *TMM*, 18(3): 405–417.
- Zhang, Y.; Zhang, Y.; Zhang, J.; Wang, H.; and Dai, Q. 2015c. Single image super-resolution via iterative collaborative representation. In *Proc. Pacific-Rim Conf. Multimedia*, 63–73.
- Zhang, Y.; Zhang, Y.; Zhang, J.; Wang, H.; Wang, X.; and Dai, Q. 2015d. Adaptive local nonparametric regression for fast single image super-Resolution. In *Proc. IEEE Int. Conf. Visual Commun. Image Process.*, 1–4.
- Zhang, Y.; Zhang, Y.; Zhang, J.; Xu, D.; Fu, Y.; Wang, Y.; Ji, X.; and Dai, Q. 2017d. Collaborative Representation Cascade for Single Image Super-Resolution. *IEEE Trans. Syst., Man, Cybern., Syst.*, PP(99): 1–11.
- Zhao, W.; Bai, L.; Rao, Y.; Zhou, J.; and Lu, J. 2024. Unipe: A unified predictor-corrector framework for fast sampling of diffusion models. In *NeurIPS*.
- Zhao, Y.; Wang, R.; Wang, W.; and Gao, W. 2015a. High resolution local structure-constrained image upsampling. *TIP*.
- Zhao, Y.; Wang, R.; Wang, W.; and Gao, W. 2015b. Multi-level modified finite radon transform network for image upsampling. *TCSVT*, PP(99): 1–1.
- Zheng, H.; Nie, W.; Vahdat, A.; Azizzadenesheli, K.; and Anandkumar, A. 2023. Fast sampling of diffusion models via operator learning. In *ICML*, 42390–42402. PMLR.
- Zhou, B.; Andonian, A.; Oliva, A.; and Torralba, A. 2018. Temporal relational reasoning in videos. In *ECCV*.
- Zhou, S.; Zhang, J.; Zuo, W.; and Loy, C. C. 2020a. Cross-Scale Internal Graph Neural Network for Image Super-Resolution. In *NeurIPS*.
- Zhou, S.; Zhang, J.; Zuo, W.; and Loy, C. C. 2020b. Cross-Scale Internal Graph Neural Network for Image Super-Resolution. In *NeurIPS*.
- Zhu, X.; Hu, H.; Lin, S.; and Dai, J. 2019. Deformable convnets v2: More deformable, better results. In *CVPR*.
- Zhu, Z.; Guo, F.; Yu, H.; and Chen, C. 2014. Fast single image super-resolution via self-example learning and sparse representation. *TMM*, 16(8): 2178–2190.

- Zibetti, M. V. W.; and Mayer, J. 2007. A robust and computationally efficient simultaneous super-resolution scheme for image sequences. *TCSVT*.
- Zoph, B.; and Le, Q. 2017. Neural Architecture Search with Reinforcement Learning. In *ICLR*.
- Zou, W. W.; and Yuen, P. C. 2012. Very low resolution face recognition problem. *TIP*.